

Final Report

Quantum Mechanics Calculation: Asymmetric Phosphine for Methanol Carbonylation

Hirihattaya Phetmung

Alain Dedieu

August 2003



Final Report

Quantum Mechanics Calculation: Asymmetric Phosphine for Methanol Carbonylation

Hirihattaya Phetmung

Alain Dedieu

August 2003

ABSTRACT

This work presents the quantum mechanics calculation based on density functional theory (DFT) for the design of new asymmetric diphosphine ligands. Complexes of this ligand can be expected to combine high catalytic activity with thermal stability under the mind conditions of methanol carbonylation process.

Chapter 1 introduces quantum mechanics, asymmetric/unsymmetric diphosphine ligand, methanol carbonylation cycle and homogeneous catalysis.

Chapter 2 provides the literature review.

Chapter 3 presents scope, aim, methodology and apparatus.

Chapter 4 presents the design and study of new asymmetric diphosphine ligands, which contain this asymmetric diphosphine ligand 1.1 which can be a promoter for methanol carbonylation. Because 1.1 has a chiral center with electron withdrawing group and electron donating group. This would be the reason that the different trans-influence and trans effect of complex type "Rh(L)L'(1.1)" would favor the formation of different isomers. Complex 1.5 is the most stable isomer among its four isomers. It cans notices that the stereochemistry at rhodium in which the P(Me)₂ trans to the CO and the PF₂ lies trans to the Me group are preferred. The presence of strong electronegativity fluorine atoms in PF₂ makes them weak σ-donors but much stronger π - acceptors and the presence of Me groups in P(Me)₂ makes them stronger σ -donors but much weaker π -acceptors, with confirming by the Rh-P bond distances. The electronic property is in a good agreement. All considered complexes adopt a square-planar geometry. The molecular orbital confirmed that the d_z^2 orbital is lower energy than d_x^2 orbital as expected for a low-spin d^8 orbital Rh (I) configuration. In a homogeneous methanol carbonylation process as developed by Forster, the outer processes involve organometallic compounds. The process made up of some four separation stoichiometric reactions, namely the oxidative addition, migratory insertion, CO ligand insertion and reductive elimination. The full catalytic cycle of asymmetric diphosphine rhodium complex 1.5 methanol carbonylation process are investigated. The investigation involves consideration of many possible structures of reaction intermediate. Isomer 1.5 is formed to be the initial catalytically active species. The interaction with the substrate CH₃I results in the formation of the six coordinated complexes N1 and N2. Later, they transform into the isomeric five coordinated acetyl complexes O3 and O4, as the result of migratory insertion process. Isomers O3 and O4 react rapidly with CO to form the six coordinated dicarbonyl complexes P5 and P6. Finally, the acetyl iodide hydrolysis leads to the formation of the target product, acetic acid. By consideration of the difference of energy (AE) values, the calculated equilibrium constant confirmed the possibility to make this model 1.5.

Chapter 5 presents the investigation of asymmetric rhodium catalysis 1.3 as the starting material for the methanol carbonylation cycle. Again, the outer four process are investigated. From the optimization data, the methyl iodide oxidative addition to the four coordinated reactant 1.3 is six coordinated isomers B5. The CO migratory insertion of octahedral isomers B5 yield the square pyramidal structures C2 and C3. The product of CO ligand addition to the five coordinated isomers C2 and C3 are six coordinated acetyl structures D5 and D6 which also are the precursor of the last reaction step, acetlyiodide elimination. In this last reaction, the six coordinated isomers D5 and D6 transform into square planar isomer 1.3. As regard the optimization energy, the methanol carbonylation process can separate into 2 routes. The first one is 1.3+Me \rightarrow B5 \rightarrow C3 +CO \rightarrow D6. The second route is 1.3+MeI \rightarrow B5 \rightarrow C2 +CO \rightarrow D5. The reaction energy of these two steps is about the same. This is confirmed that the oxidative addition of methyl iodide to 1.3 may have only isomer B5. Form the enthalpy energy, the product from oxidative addition to migratory insertion change rapidly, indicating from the similar energy. Once again, the difference of energy (Δ E) values are used to calculated equilibrium constant and confirmed the possibility to make this model 1.3.

To my dearest and greatest Dad

ACKNOWLEDGEMENTS

This research would not have been possible without the continuous guidance of my mentor Prof. Dr. Alain Dedieu (University Louis Pasteur (Strasbourg)) to whom I will be grateful.

I would like to acknowledge the Thaksin University staffs, Associate Prof. Dr. Somboon Chitapong, the President of Thaksin University, to Dr. Somsak Chokenukul and to Dr. Pradit Tungsakul for their support and good advice. A lots of thanks to Kun Chadatip Channilla and Ajarn Varakorn Wispan for their hospitality and support and also to the Department of Chemistry for providing me such a research facility and a place where to do a research.

I gratefully thank Prof. Dr. Tom Ziegler, the University of Calgary, Canada, Assist. Prof. Dr. Vuttichai Parasut and Assist. Prof Dr. Supot Hannongbua, Chulalongkorn University, and to Prof. Dr. Michael Probst from University of Innsburgh, for their helpful suggestion.

I would like to thank my students in my laboratory from the past to the present, especially to Munee for her contribute help in checking my data.

An enormous thanks to "the Thailand Research Fund" for creating my opportunity to explore the world of molecular modeling and for a research grant support.

My biggest debt is to my family, especially my lovely mom, for their love and support at all times. ขอบพระอุณมากละ

Finally, the good value of this work is for every name appearing in this research. Of course, all mistakes in this work are mine.

MEMORANDUM

The work described in this research was carried out in the Department of Chemistry at the Thaksin University between September 2001 and August 2003. Unless otherwise acknowledged within the text, it is the original work of the author. In addition, any views expressed in this Research are those of the author, and not of the Thailand Research Fund.

Hirihattaya Phetmung Thaksin University August 2003

CONTENTS

| | | | age |
|------------------|----------|--|-------|
| | | | |
| | | | |
| | | | |
| Memorandum | l | | iv |
| | | | |
| List of Figure | S | | .viii |
| List of Tables | | | X |
| List of Schem | es | | xii |
| Abbreviations | S | | .xiii |
| Chapter 1: | Introd | luction | |
| 1.1.Introducti | on to Q | nantum Mechanics Calculation | 1 |
| | 1.1.1 | An Overview | 1 |
| | 1.1.2 | Quantum Mechanics Methods | 2 |
| | 1.1.3 | History and Principles of Quantum Mechanics | 2 |
| | 1.1.4 | Ab initio Hartree-Fock Methods | |
| | 1.1.5 | Effective Core Potential Methods | 3 |
| | 1.1.6 | Correlated ab initio Methods | 4 |
| | 1.1.7 | Semi-empirical Methods | 4 |
| | 1.1.8 | Density Functional Theory | 5 |
| | 1.1.9 | Basis Sets | 5 |
| | 1.1.10 | Open and Closed Shell | 6 |
| | 1.1.11 | Geometry Optimization | 6 |
| | 1.1.12 | The Potential Energy Surfaces | 6 |
| | 1.1.13 | Locating the Global Minimum and Conformational Sampling. | 7 |
| | 1.1.14 | Advantage of DFT | 7 |
| 1.2 Introduction | on to As | symmetric Phosphines | 7 |
| | 1.2.1 | History | 7 |
| | 1.2.2 | General Information. | 7 |
| | 1.2.3 | Asymmetric Phosphine/Unsymmetric Phosphine | 8 |
| | 1.2.4 | Coordination complexes of Asymmetrical diphosphines | 9 |
| | 1.2.5 | Electronic and Steric Effects in Phosphines | |
| | | 1.2.5.2 Steric Effects in Phosphines | |
| 1.3 Introduction | on to Me | ethanol Carbonylation | |
| | | Methanol and Carbon Monovide | |

| | 1.3.2 | The Methanol Carbonylation | 13 |
|--------------------|---------------|--|-----|
| | 1.3.3 | 3 The Methanol Carbonylation Produces Acetic Acid | 14 |
| 1.4 Int | roduction to | Homogeneous Catalysis by Transition Metal Phosphine Complex | 16 |
| | 1.4. | Chelating Phosphines in Homogeneous Catalysis | 16 |
| 1.5 Re | ferences | | 19 |
| Chapt | er 2: Lite | rature Review | 22 |
| 2.1 Q | uantum Mecl | nanics Calculations: A Theoretical Study | .22 |
| 2.2 As | symmetric D | iphosphines in Methanol Carbonylation:An Experimental Study2 | 24 |
| 2.3 Re | eferences | | 29 |
| Chapt | ter 3: Sco | pe, Aims and Methodology | 31 |
| 3.1 Sc | cope and Ain | ns | 31 |
| 3.2 M | ethodology | | 32 |
| | 3.2. | l Designed Structures | 32 |
| | 3.2.2 | 2 Computational Methodology | 33 |
| 3.3 A ₁ | pparatus | | 34 |
| | 3.3. | 1 High Performance Computer | 34 |
| | 3.3.2 | 2 Softwares | 34 |
| 3.4 Re | eferences | | 35 |
| Chapt | er 4: Res | ults and Discussion-1 | 36 |
| 4.1 To | Find the Be | st Calculation Type for Such These Structures | 36 |
| 4.2 To | Find the Mo | ost Stable Structure | 38 |
| | 4.2.1 | The Study of Ligand 1.1 and Cation 1.2 | 38 |
| 4.3 Th | ne Optimizati | on Energy for All Four Rhodium Structures | 42 |
| | 4.3. | The Optimization of Isomers 1.3 and 1.4 | 42 |
| | 4.3.2 | The Optimization of Isomers 1.5 and 1.6 | 43 |
| | 4.3.3 | The Optimization of Isomers 1.3 and 1.5 | 45 |
| 4.4 To | Do Full Opt | imization of Methanol Carbonylation Cycle (1.5) | 48 |
| | 4.4. | Initial four-coordinated Complex 1.5 | 48 |
| | 4.4.2 | 2 Six-coordinated Complex N | 48 |
| | 4.4.3 | Five-coordinated Complex O | 51 |
| | 4.4.4 | Six-coordinated Complex P | 54 |
| 4.5 As | ymmetric Di | phosphine for Methanol Carbonylation Cycle | 56 |
| | 4.5. | Overall Methanol Carbonylation cycle | 56 |
| | 4.5.2 | 2 Oxidative Addition Process | 58 |
| | 4.5.3 | Migratory Insertion Process | 59 |

| | 4.5.4 | Ligand Addition Process | 61 |
|---------------|----------|---|-----|
| | 4.5.5 | Reductive Elimination Process | 61 |
| | 4.5.6 | The Oxidative Addition and Reductive Elimination | 62 |
| 4.6 Concludin | ng Rema | arks | 63 |
| | - | | |
| Chapter 5: | Resul | t and Discussion-2 | 66 |
| 5.1 Intermedi | ate Invo | olved in the Catalytic Cycle | 66 |
| | | Initial Four-coordinated Complex 1.3 | |
| | | Six-coordinated Complex B | |
| | | Five-coordinated Complex C | |
| | | Six-coordinated Complex D | |
| 5.2 Methanol | Carbon | ylation Cycle | 73 |
| | | Oxidative Addition Process | |
| | | Migratory Insertion | |
| | | Ligand Addition Process | |
| | | Reductive Elimination Process | |
| 5.2 Concludi | | The Oxidative Addition and Reductive Elimination arks | |
| | • | airs | |
| | | | |
| Appendix A | Sumn | nary of Structures | 80 |
| Appendix B | Sumn | nary of Energies | 84 |
| Appendix C | Sumn | nary of Optimized Parameters | 87 |
| Appendix D | Sumn | nary of Standard Orientation Coordinates | 98 |
| Appendix E | Sumn | nary of Other Supporting Data | 107 |
| Appendix F | Articl | es, Conference and Presentation | 113 |

LIST OF FIGURES

| | Page |
|------------|--|
| Chapter 1 | |
| Figure 1.1 | Symmetric Phosphine Derivatives8 |
| Figure 1.2 | Asymmetric Phosphine Derivatives9 |
| Figure 1.3 | The classical view of the principal M-P bonding interactions in |
| | metal-phosphine complexes: a) P to M σ donation; b) π -backbonding |
| | from filled metal d_{xz} and d_{yz} orbitals to empty phosphorus $3d_{xz}$ |
| | and $3d_{yz}$ orbitals10 |
| Figure 1.4 | a) The geometrical definition of the cone angle11 |
| | b) The geometrical definition of the semicone angle |
| Figure1.5 | Ligand cone angle (θ) for chelating diphosphine. Note the dependence |
| | of cone angle upon the PMP bite angle(β)12 |
| Figure 1.6 | Oil Refining: Catalysts for converting crude oil to gasoline15 |
| Figure 1.7 | Possible sites for modification of phosphorus (III) ligands17 |
| Chapter 2 | No Figures |
| Chapter 3 | |
| Figure 3.1 | A ligand 1.131 |
| Figure 3.2 | Proposed the formation of different rhodium isomers31 |
| Figure 3.3 | Designed ligand 1.1, cation 1.2, and complexes 1.3, 1.4, 1.5 and 1.633 |
| Chapter 4 | |
| Figure 4.1 | The structures of complexes 1.5 and 1.6. Hydrogen atoms are |
| | omitted for clarity36 |
| Figure 4.2 | A symmetric ligand 1.1 shows the molecular orbitals. Hydrogen atoms |
| | are omitted for clarity .The energies are in au40 |
| Figure 4.3 | A rhodium cation 1.2 shows the molecular orbitals. Hydrogen atoms are |
| | omitted for clarity .The energies are in au41 |
| Figure 4.4 | The possible isomers generated by asymmetric diphosphine |
| | ligand 1.141 |
| Figure 4.5 | Some molecular orbitals of complex 1.5. Hydrogen atoms are |
| | omitted for clarity. The energies are in au46 |
| Figure 4.6 | The relative of the three types (two of which are important) of |
| | CO-Metal bonding51 |

| Figure 4.7 | The methyl iodide oxidative addition to isomer 1.5 yield | |
|-------------|---|----|
| | products N1 and N2 | 58 |
| Figure 4.8 | The migratory insertion of N1 and N2 yield O3 and O4 | 60 |
| Figure 4.9 | The CO ligand addition of O3 and O4 yield P5 and P6 | 61 |
| Figure 4.10 | The reductive elimination acetyiodide | 62 |
| Chapter 5 | | |
| Figure 5.1 | The methyl iodide oxidative addition to isomer 1.3 yield product B5 | 75 |
| Figure 5.2 | The migratory insertion of B5 into C3 and C2 | 76 |
| Figure 5.3 | The CO ligand addition of C3 and C2 yield D6 and D5 | 76 |
| Figure 5.4 | The reductive elimination acetlyiodide | 77 |
| Figure 5.5 | The relation between oxidative addition and reductive elimination | 78 |

LIST OF TABLES

| | | Page |
|------------|---|------|
| Chapter 1 | | |
| Table 1.1 | Industrial routes to acetic acid | 14 |
| Table 1.2 | Acetic acid production by carbonylation of methanol | 15 |
| Table 1.3 | Some processes catalyzed homogeneously | 16 |
| Chapter 2 | | |
| Table 2.1 | Relative rates of rhodium catalysts for methanol carbonylation | |
| | screened by Baker et al | 26 |
| Chapter 3 | No Tables | |
| Chapter 4 | | |
| Table 4.1 | Comparison of computed rhodium complexes 1.5 and 1.6 at different | |
| | levels of theory: HF/3-21G, HF/LANL2DZ, DFT/3-21G, | |
| | DFT/LANL2DZ, and typical dimensions | |
| Table 4.2 | Energies of complexes 1.5 and 1.6 | |
| Table 4.3 | The optimized parameters of 1.1 and 1.2 | 38 |
| Table 4.4 | Some atomic charges of ligand 1.1 | 39 |
| Table 4.5 | Some numbers of IR and Raman stretching frequency of ligand 1.1 | 39 |
| Table 4.6 | The geometry comparison of isomers 1.3,1.4 and reference structures | 42 |
| Table 4.7 | Number of IR and Raman CO stretching frequencies of series 1 | 43 |
| Table 4.8 | The energy of isomers 1.3 and 1.4. | 43 |
| Table 4.9 | The geometry comparison of isomers 1.5and 1.6 | 44 |
| Table 4.10 | The energy of isomers 1.5 and 1.6 | 45 |
| Table 4.11 | The geometry comparison of isomers 1.3 and 1.5 | 45 |
| Table 4.12 | The energy of isomers 1.3 and 1.5 | 46 |
| Table 4.13 | The optimization energy and relative energy of complex N series | 49 |
| Table 4.14 | The parameters of the N series with calculated bond distances | |
| | (in A°) and bond angles (in deg°) | 50 |
| Table 4.15 | Number of IR and Raman CO stretching frequencies of series N | 50 |
| Table 4.16 | The optimization energy and relative energy of complex O series | 52 |
| Table 4.17 | Calculated bond distances (in A°) and bond angles (in deg°) of | |
| | migration process | 52 |
| Table 4.18 | Number of IR and Raman CO stretching frequencies of series O | 53 |
| Table 4.19 | The optimization energy and relative energy of complex P series | 54 |

| Table 4.20 | Calculated Bond distances (in A°) and Bond Angles (in deg°) of |
|------------------------|--|
| | ligand addition process55 |
| Table 4.21 | Number of IR and Raman CO stretching frequencies of series P55 |
| Table 4.22 | The optimization energies of the most stable isomers from each |
| | step including molecules of CO, CH ₃ I and CH ₃ COI55 |
| Table 4.23 | The overall energies of each reaction in au and kcal/mol58 |
| Table 4.24 | Kinetic data for oxidative addition reaction of MX(CO)(PR ₃)59 |
| Chapter 5 | |
| Table 5.1 Table 5.2 | The optimization energy and relative energy of complex B series67 The parameters of the N series with calculated bond distances |
| | (in A°) and bond angles (in deg°)68 |
| Table 5.3 Table 5.4 | The optimization energy and relative energy of complex C series 69 Calculated bond distances (in A°) and bond angles (in deg°.) of |
| | migration process69 |
| Table 5.5 | The optimization energy and relative energy of complex O series71 |
| Table 5.6 | Calculated bond distances (in A°) and bond angles (in deg°.) of ligand addition process |
| Table 5.7 | The optimization energies of the most stable isomers from each step including molecules of CO, CH ₃ I and CH ₃ COI |
| Table 5.8 | The overall energies of each reaction in au and kcal/mol |

LISTS OF SCHEMES

| | Page |
|------------|--|
| Chapter 1 | |
| Scheme 1.1 | Summary of industrial methanol conversion reactions |
| Chapter 2 | |
| Scheme 2.1 | Catalytic cycle of the rhodium-catalyzed methanol carbonylation25 |
| Scheme 2.2 | The methanol carbonylation cycle catalyzed by |
| | Rh[Ph ₂ PCH ₂ P(S)Ph ₂](CO)I27 |
| Scheme 2.3 | Synthesis rhodium complexes with asymmetrical diphosphine |
| | ligands28 |
| Chapter 3 | |
| Scheme 3.1 | Proposed catalytic cycle for methanol carbonylation in rhodium |
| | complexes32 |
| Chapter 4 | |
| Scheme 4.1 | The most stable optimization structures involve the methanol |
| | carbonylation cycle56 |
| Scheme 4.2 | The full optimized methanol carbonylation cycle using only |
| | the lowest optimization energy57 |
| Scheme 4.3 | The purposed mechanism of oxidative addition process |
| Scheme 4.4 | The purposed mechanism of migratory insertion process60 |
| Scheme 4.5 | The relative between migratory insertion and ligand CO addition61 |
| Scheme 4.6 | The route of reductive elimination62 |
| Scheme 4.7 | The relation between oxidative addition and reductive elimination62 |
| Chapter 5 | |
| Scheme 5.1 | The most stable optimization structures involve the methanol carbonylation cycle |
| Scheme 5.2 | The full optimization methanol carbonylation cycle using only |
| Scheme 5.3 | the lowest optimization energy74 The full optimization methanol carbonylation cycle using only |
| | the second lowest optimization energy |

ABBREVIATIONS

AM Austin Model
atm Atmosphere
AO Atomic Orbital
au Atomic unit

B3LYP Beck's three-parameter and Lee-Yang-Parr non-local correlation

functional

cod Cis-1,5-cyclooctadiene
CPK Corey-Pauling-Koltun

DFT Density Functional Theory

dppe 1,2-bis(diphenylphosphino)ethane

dppms Bis(diphenylphosphine)methanesulfide

ECP Effective Core Potential

EHT Extended Hückel Theory

ev Electron volt

GTO Gaussian Type Orbital

HE Half-electron
HF Hartree Fock

HF-SCF Hartree-Fock Self Consistent Field HOMO Highest Occupied Molecular Orbital

IR Infra-red

LCAO Linear Combination of Atomic Orbitals
LUMO Lowest Unoccupied Molecular Orbital

Me Methyl

MM Molecular Mechanics

NMR Nuclear Magnetic Resonance

PES Potential Energy Surface

POS Point On a Sphere

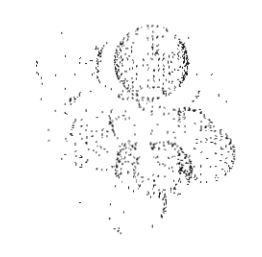
QM Quantum Mechanics

RHF Restricted Hartree Fock

RHF - ECP Restricted Hartree Fock-Electron Core Potential

SCF Self Consistent Field
 STO Slater Type Orbital
 UFF Universal Force Field
 δ Chemical shift (in ppm)

{1H} Proton decoupled





CHAPTER 1 INTRODDUCTION





Chapter 1: Introduction

Organometallic chemistry, which involves metal complexes containing direct metal-to-carbon bonds, has grown since the early 1950s at an almost exponential rate, mostly owing to the development of an impressive array of highly sophisticated apparatus of which in particular NMR and single-crystal X-ray equipments have been invaluable. Theoretical studies of the bonding in metal compounds and of the course of reaction pathways have not only contributed to new knowledge, but also to the purposeful design of complexes and their use in stoichiometric and catalytic reactions.

Although fortunate surprises do occur frequently, our theoretical knowledge has increased to a level where we have a deep insight into the steric and electronic properties of ligands and of their complexes. Therefore, we are now, to a certain extent, able to design ligands and to control reactions occurring on metal centers in complexes.

As this work is concerned with the design of new ligands involved in the methanol carbonylation. This chapter 1 is divided into 4 main parts:

- 1.1 Introduction to quantum mechanics calculation
- 1.2 Introduction to asymmetric phosphines
- 1.3 Introduction to methanol carbonylation
- 1.4 Introduction to homogenous catalysis by transition metal complex

1.1 Introduction to Quantum Mechanics Calculation

1.1.1 An Overview

Computational Chemistry is embodied in nearly every aspect of chemical research, development, design and manufacture. It has a broad range of applications, from molecular modeling to simulation and control of chemical process.

Molecular Modeling is an area of research in which computer hardware and software are used to simulate chemical processes or to compute chemical properties. This discipline has advanced tremendously in the past few decades and is now one of the main stays of modern industrial and academic chemistry. The computer serves as an instrument to solve real-world chemical research problems, much like the diffractometer is the tool of X-ray crystallography or the spectrometer is the tool of nuclear magnetic resonance spectroscopy. Methods in computational chemistry are now used to solve a broad range of chemical problems, including structural chemistry, molecular spectroscopy, mechanistic studies, biotechnology (protein and drug design) and materials science (polymer, catalysis, metal, solid surfaces, etc.

Catalytic design is one of such example that clearly illustrates the promise and challenges of computational chemistry. Almost all chemical reactions of industrial or biochemical significance are catalytic. Yet, catalysis is still more of an art (at best) or an empirical fact then a design science. But this is sure to change. A major obstacle to the commercialization of homogeneous catalysts is that they are often difficult to

Chapter 1 Introduction

separate from the reaction products and the solvent. It is attempting to tackle this in a number of different ways.

Nowadays, computational chemistry especially theoretical studies such as quantum mechanics calculations are used as a tool to understand mechanism and reaction. There are a lot of papers reported about catalyst used in fuel procedure. Asymmetric phosphine catalysis involving organometallic species is undergoing rapid development and it is clear that phosphine ligands are control to this growth.

1.1.2 Quantum Mechanics Methods

Quantum mechanics calculations, in particular electronic structure calculations, play a key role in modern-day chemistry. In general, they are now being used routinely in support or lieu of experiment to further the understanding chemical system known structures of fragments. They may be divided into four distinct classes 1: ab initio Hartree-Fock methods, ab initio correlated methods, semi-empirical methods and density functional methods. Within each class, many variations may occur in, for example, the details of parameterized for semi-empirical methods, variation of basis sets and level of inclusion of electron correlation for ab initio methods, choices of functional for density functional methods.

1.1.3 History and Principles of Quantum Mechanics

Quantum Mechanics (QM) is the theory of nuclear, atomic and molecular systems. The theory of quantum mechanics originated in the 1920s. Initially the aim of quantum mechanics was the calculation of all chemical interactions, thereby making experiments almost obsolete. Hartree performed the first reliable calculations in the 1930s, using a hand calculator and applying the Self Consistent Field (SCF) method. However, it is based on the Schrödinger equation (Equation 1.1), the solution of which consists of the wave function of the system of particles.²⁻³

$$H\Psi = E\Psi$$
 1.1

where H is Hamiltonian Ψ is the wave function E is the energy of the system

The Hamiltonian operator H is applied to the wavefunction Ψ to give the energy E multiplied by the wavefunction. Only certain solutions are allowed and hence this is an eigenvalue equation where E is the eigenvalue and Ψ the eigenvector. The square of the wavefunction is the physically observable electron density.

The Schrödinger equation can not be solved analytically without approximations.⁴ Time independence of the Hamiltonian operator and neglect of relativistic effects on the electron mass are assumed. The Born-Oppenheimer approximation of fixed nuclei is used.⁵ Electrons are added to these nuclei and the energy levels of the resulting atomic orbitals are calculated. A Linear Combination of the Atomic Orbitals gives the Molecular Orbital energies (LCAO-MO method). Since each addition perturbs the old system, iterative calculations have to be performed until the answer for the total energy is self-consistent (SCF). The electron

distribution on the molecule can be calculated from the wavefunction. The most common equations approximating the Schrödinger equation are the matrix equations defined by Hartree-Fock-Roothaan (Equation 1.2).

$$FC = SCE$$
 1.2

F is the Fock operator whose matrix elements are constituted by one-electron terms and two electron repulsions. S is the overlap matrix, E the energy and C is the matrix holding the coefficients of the atomic orbitals in the molecular orbitals. An initial guess of these latter coefficients or contributions is needed to construct the first Fock matrix. After iterative solution the new coefficients are within a convergence criterion from the old or input coefficients and a SCF is achieved. Quantum mechanical computations require only nuclear coordinates and electronic state that have to be defined.

1.1.4 Ab initio Hartree-Fock Methods

Chapter 1

If solutions are generated without reference to experimental data, the method are call "ab initio". ⁷ The solutions of the Schrödinger equation (equation 1.1) use a series of mathematical approximations. Ab initio methods use no experimental parameters in their computations, unlike semi-empirical methods. Instead, their computations are based solely on the laws of quantum mechanics, the first principles referred to in the name ab initio and on the values of a small number of physical constants, i.e. the speed of light, the masses and charges of electrons and nuclei and Planck's constant.⁸

Computation of all integrals or 'ab initio' quantum mechanics gives the most accurate results. The obtained accuracy, however, depends on the number of gaussian functions that replace the Slater type function that depicts the actual shape of the orbital. These basis sets for calculation show increasing accuracy going up from STO-3G (where a Slater Type Orbital is replaced by 3 Gaussians).

Ab initio techniques have been used to study transition-metal complexes and other inorganic systems. For example, work on olefin hydrogenation catalysed by the model rhodium complex RhCl(PH₃)₃ were carried out using HF-SCF level. This work confirmed that oxidative addition of H₂ to RhCl(PPh₃)₂ takes place ca. 4 times faster than to RhCl(PH₃)₃ and that excess PPh₃ inhibit the catalysis, thus indicating that the associative mechanism is not operative.⁹

1.1.5 Effective Core Potential Methods

Since the cost of the *ab initio* calculations rises rapidly with the number of electrons, the innermost electrons and nucleus are frequently replaced with an effective core potentials (ECP), thus reducing the calculation to a more computationally feasible valence electron problem. In addition, one can incorporate into the ECP the relativistic effects, which are important in heavy atoms.

The ECP has been used in reaction studies of transition-metal complexes such as carbonyl insertion in [Pt(CH₃)(H)(CO)(PPh₃)]. In this study, optimisation the

structures of the reactant and product [Pt(COCH₃)(H)(Ph₃)] at the RHF-ECP level shows that transition state is three-centred and that the methyl group migrates toward the CO group.

1.1.6 Correlated ab initio Methods

The term "electron correlation energy" is usually defined as the difference between the exact nonrelativistic energy of the system and the Hartree-Fock self-consistent field energy. Electron correlation effects are particularly important in chemical bond formation.

One of the most challenging problems in ab initio quantum chemistry is to calculate the bond energies of molecules within chemical accuracy (within 0.1 eV or 2 kcal/mol). Electron correlation methods such methods as HF and the Møller-Plesset partitioning (MP2, MP3 and MP4) yield electron correlation energies accuracy such as bond energy of N₂ with an error of ~1.0-1.5 kcal/mol. HF and MP2 methods are successful in mechanism studies. Such as the recent study of the structure and reactivity of oxidative addition of H₂ and CH₄ to trans-and cis-[RhCl(CO)(PH₃)₂] using HF and MP2.

1.1.7 Semi-empirical Methods

The need for faster calculations on larger molecules started development of the semi-empirical quantum mechanical methods.²⁰ Semi-empirical methods may be defined as approximate procedures which rely on a set of empirical parameters to calculate the wave function of valance electrons only. The inner shell electrons are treated together with the nucleus, as an unpolarisable core.²⁰⁻²¹

The amount of neglect of the diatomic differential overlap integrals is the major discrimination between most semi-empirical methods. Among a variety of semi-empirical methods AM1, PM3 and Extended Hückel methods are popular. AM1 (Austin Model 1) was developed by Steward et.al.²²⁻²⁴ The method is based on the linear combination of atomic orbitals for a solution of Hartree-Fock equations. Overall, AM1 was a significant improvement over MNDO and many of the deficiencies associated with the core repulsion were corrected. PM3 is the third parameterisation of MNDO.²²⁻²⁵ The PM3 Hamiltonian contains essentially the same elements as that for AM1 but the parameterisation is different. PM3 used an automated parameterisation procedure derived by Stewart.²³⁻²⁵ By contrast many parameters in AM1 were obtained by applying chemical knowledge and "intuition". As a consequences, some of the parameters have significantly different values even though both methods used the same functional form and they both predict various thermodynamics and structural properties to approximated the same level of accuracy.

Both AM1 and PM3 are based on MNDO but PM3 technique offers the best parameterisation for phosphorus, although both use the same functional form.

Chapter 1 5 Introduction

1.1.8 Density Functional Theory

Density functional theory has proven itself to be a powerful tool in the elucidation of complex chemical phenomena, especially in transition metal systems, which are key factors in homogeneous catalysis.

Density Functional Theory (DFT) is an alternative approach to the calculation of the electronic structure of atoms and molecules which complements traditional *ab initio* methods. The approach is based on a theory presented by Hohenberg and Kohn.²⁶

Walter Kohn was awarded the 1998 Nobel Prize in Chemistry "for his development of the density-functional theory. W.Kohn's theoretical work has formed the basis for simplifying the mathematics in descriptions of the bonding of atoms, a prerequisite for many of today's calculations. DFT, standing as it does at the boundary between the disciplines of physics, chemistry, and materials science, is a great mixer".

In DFT²⁶ the system of interest has N electrons and a fixed set of nuclear positions, the nuclei gives rise to an external potential, v(r), in which the electrons move and repel each other. The time-independent ground-state electronic wave function may be obtained by solution of the Schrödinger equation. The wave function is determined by N and v, as is the electron energy: E[N, v]. The electron density, $\rho(r)$ is N times the integral of the square of the wave function over all electronic space and integral at the square of the wave function over all electronic space and spin coordinates. The density determines v(r) and v(r) uniquely; hence $v(r) = E[\rho]$. Provided v(r) = v(r) is at a minimum when v(r) = v(r) is the correct ground-state density. The total electronic energy is given by

$$E[\rho] = F[\rho] + \int v(r)\rho(r)d(r)$$
 1.3

where $F[\rho]$ is the universal function of ρ or the sum of the kinetic energy functional $T[\rho]$

In practice, a DFT calculation is in many way like a traditional HF one, and the final outcome is a set of molecular orbitals. Pure DFT methods are defined by pairing an exchange functional with a correlation functional. For example, the well known BLYP functional pairs Becke's gradients-corrected exchange functional with the gradient-corrected correlation functional of Lee, Yang and Parr.²⁷

Many studies done by Ziegler confirmed that this method is suitable for molecular structures, potential energy surfaces and conformational analysis, transition-state structures and reaction profiles.²⁸ A study done at approximate DFT method on *cis*-and *trans*-[RhCl(CO)(PH₃)₂], shows that *trans*-[RhCl(CO)(PH₃)₂] is about 9 kcal/mol more stable than *cis*-[RhCl(CO)(PH₃)₂.]²⁹

1.1.9 Basis Sets

A basis set is a mathematical representation of molecular orbitals within a molecule. The basis set can be interpreted as restricting each electron to a particular

Chapter 1 6 Introduction

region of space. Larger basis sets impose fewer constraints on electrons and more accurately approximate exact molecular orbitals.

There are two different types of basis sets³⁰ Slater Type Orbitals (STO) and Gaussian Type Orbitals (GTO). STO's are exponential atomic orbitals (AO) based on Slater's Rules.³¹ GTO's are a sets of AOs of gaussian form.³² Both offer mathematical description of the atomic orbitals which in turn are combined to approximate the total electronic wave function. There are three different classes of basis set: minimal, split valence and polarised basis sets.

1.1.10 Open and Closed Shell.

Two main types of calculations are employed. The restricted Hartree-Fock (RHF) calculations on closed shell systems, where all orbitals are empty or have paired electrons and the unrestricted Hartree-Fock calculations (UHF) for open shell systems with one or more unpaired electrons. In the latter case the orbitals are split to account for electrons with and β spin state. The doublet spin state is reflected by an expectation value. The expectation value for a doublet is 1/2 * (1/2 + 1). Higher values point at spin contamination. Besides an UHF treatment for open shell systems, also the half-electron (HE) method has been used with success.

1.1.11 Geometry Optimization

Geometry optimization methods³⁰ normally try to attempt to locate minima on the PES. Optimizations to minima are also called *minimizations*. At both minima and saddle points, the first derivative energy known as the *gradient*, is zero. Since the gradient is the negative of the forces, the forces are also zero at such a point. A point on the PES where the force are zero is called a *stationary point*. All successful optimizations locate stationary points, although not always the one that was intended.

Most optimization algorithms also estimate or compute the value of the second derivative of the energy with respect to the molecular coordinates, updating the matrix of force constants (known as the *Hessian*). These force constants specify the curvature of the surface at the point, which provides additional information useful for determining the next of the stationary point (minimum, saddle or maximum).

Calculations investigate a molecular system having a specified geometric structure. Structure changes within a molecule normally produce differences in its energy and other properties. The way the energy of a molecular system varies with changes in its structure is specified by its potential energy surface.

1.1.12 The Potential Energy Surfaces

The potential energy surface (PES) is a mathematical relationship linking molecular structure and the resultant energy. For a diatomic molecule, it is a two-dimensional plot with the internuclear separation on the X-axis and the energy at that bond distance on the Y-axis, producing a curve. For larger systems, the surface has as many dimensions as there are degrees of freedom with in molecule, plus one (for the energy).

Chapter 1 7 Introduction

1.1.13 Locating the Global Minimum and Conformational Sampling

Methods such as sleepest descent, conjugated gradient and Newton-Raphson can only locate the nearest minimum which is normally a "local minimum", when starting from a given set of variables. In some cases, the interest is in the lowest of all such minima, the "global minimum", in other cases it is important to sample a large set of local minima. consideration, for example, a determination of the lowest energy conformation of butane, there are three conformations, one *anti* and two *gauches* (which are symmetry equivalent). These minima may be generated by starting optimisations from three torsion angles separated by 120°.

1.1.14 Advantage of DFT

Density functional theory (DFT) provides a simple and computationally efficient scheme for dealing with the notoriously difficult many-body problem. When applied to systems of electrons, for example, the total energy of the interacting electron gas can be expressed entirely in terms of the electron density - a one-body quantity - and there is no need to construct the actual many-body wavefunctions, resulting in tremendous savings in the computer effort needed to resolve a particular problem.

DFT is at the heart of the tremendous effort that is currently being spent on solving atomic-scale problems³³ related to:

- 1. Drug design
- 2. Micro-device fabrication and ionic transport through membranes to mention a few examples; this was largely motivated by the unification of DFT and molecular dynamics, initially proposed by Roberto Car and Michele Parrinello.
- 3. Homogenous catalysis. ²⁸⁻²⁹ DFT has proven itself to be a powerful tool in the elucidation of complex chemical phenomena, especially in transition metal systems, which are key factors in homogeneous catalysis. Applications will also be presented of olefin polymerization by metallocenes and derived types, carbonylation of C-H bonds by a Vaskatype catalyst and copolymerization of CO and ethylene by a Pd (II) catalyst.

1.2 Introduction to Asymmetric Phosphines

1.2.1 History

Tertiary organic phosphines have found wide applications in homogeneous catalysis. They were discovered around the middle of the last century and their ability to combine with heavy metal salts to form coordination complexes was noted almost immediately. However, the application of their metal complexes to homogeneous catalysis came only after the lapse of about 100 years.³⁴

1.2.2 General Information

Phosphine ligands have the general formula PR_3 where R = alkyl, aryl, H, halide etc. Closely related are phosphite ligands which have the general formula

Chapter 1 8 Introduction

P(OR)₃. Both phosphines and phosphites are neutral two electron donors that bind to transition metals through their lone pairs. There are many examples of polydentate phosphine ligands, some common examples of which are shown below.

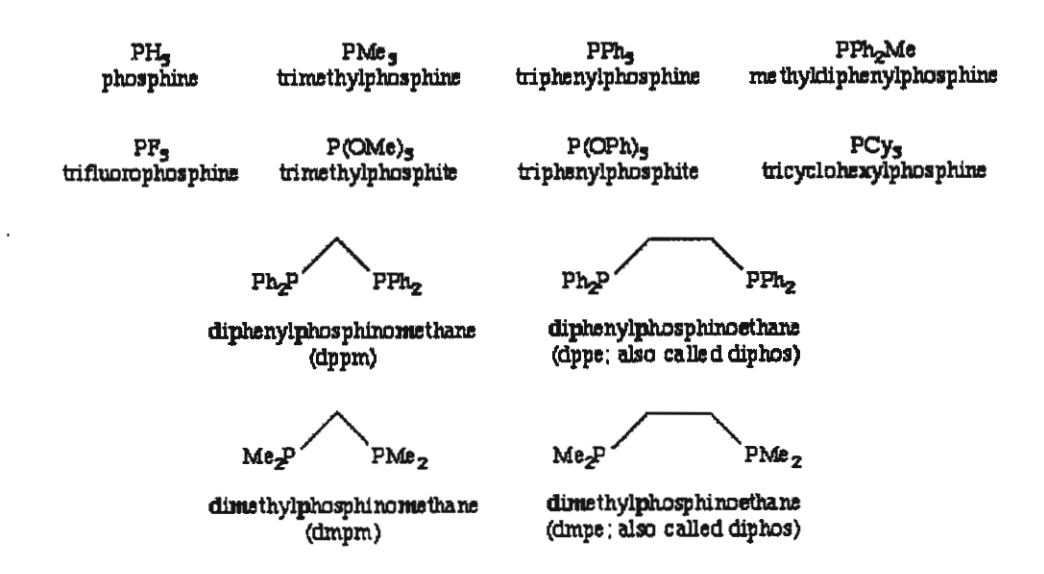


Figure 1.1 Symmetric Phosphine Derivatives

1.2.3 Asymmetric Phosphine/Unsymmetric Phosphine

Asymmetric phosphine has a chiral center which contains a atom that is surrounded by four different groups, allowing for isomers. Phosphine can complex to transition metals through the lone pair of electrons on the phosphorus atom. Replacing the hydrogen atoms with other groups can give chiral ligands, and so chiral catalysts.

A wide range of unsymmetrical diphosphines were prepared by substituting diphenylphosphine with different secondary phosphines.³⁵ Later, Grim et al.³⁶ developed the synthesis of unsymmetrical ditertiary phosphines of the type $Ph_2PCH_2CH_2PPhR$. Diphosphines have a chiral centre and several have been resolved as single enantiomers.³⁷ Functionalised derivative have also been reported.³⁸ The diphosphine was the first example of a detertiary phosphine with chirality in the terminal group as well as at phosphorus.³⁷ This enable the two diastereomers to be separated by fractional crystallisation and their Rh(I) complexes were used as asymmetric hydrogenation catalysts for α -(acylamido) cinnamic acid with moderated e.e.'s (31-88%).

The success of development asymmetric diphosphines, more recently, by Shell³⁹ on the stability of the aryl anoin formed after cleavage. With electron-withdrawing groups present in the elimianated aryl anion, good yields are obtained.

Furthermore, a variety of chiral phosphine transition metal complexes have been synthesized; these phosphine-metal complexes are stereogenic and can function as stereospecific catalysts. Some typical phosphine ligands are shown below:

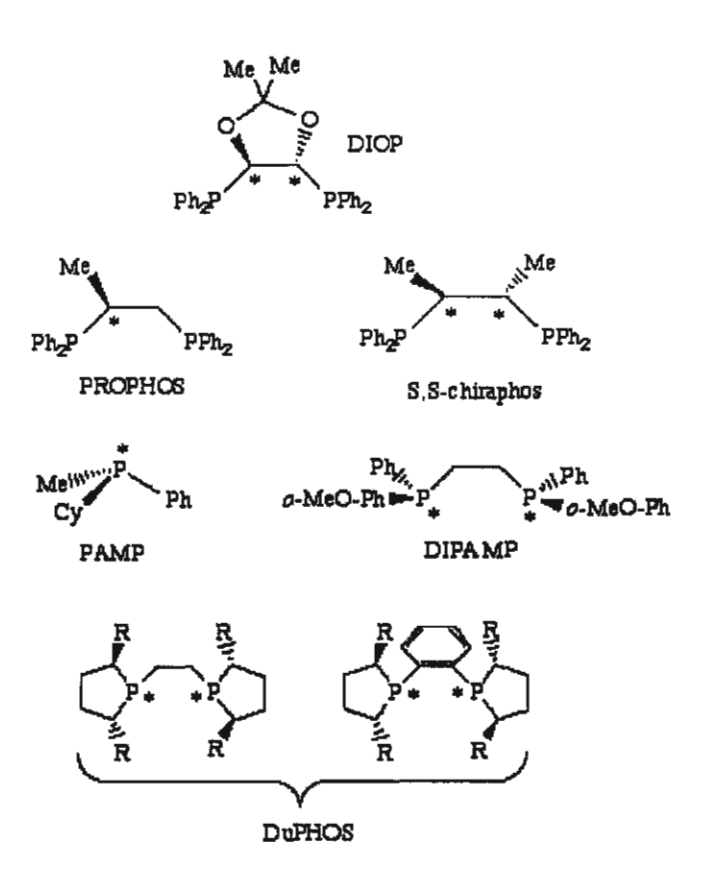


Figure 1.2 Asymmetric Phosphine Derivatives

1.2.4 Coordination complexes of Asymmetrical diphosphines

Transition metal complexs of unsymmetrialcal diphosphines have previously been synthesized in order to investigate metal-ligand bonding⁴⁰ and to increase complex solubility.⁴¹ By having different organic groups on the phosphorus donor, the effect of different steric or electronic properties can be investigated by IR, NMR etc. Grim et al.⁴² first reported on the chromium, molybdenum and tungsten complexes of unsymmetrical diphosphine Ph₂PCH₂CH₂PPhR and Ph₂PCH₂CH₂PR₂ (R = alkyl).

The complex using similar unsymmetrical diphosphines, in which the potentially bidentate ligand behaves as a monodentate ligand was prepared. In this case, linkage isomerism is possible since the two phosphorus atoms are chemically different.

The majority of complexes previously reported for unsymmetrical diphosphines all contained equivalent ligands *trans* to the diphosphine. This means only one isomer is possible. Similar complexes were prepared by us for comparison but complexes with different substituents were also prepared *e.g.* [PdClMe(diphos)], [PtClMe(diphos)] and [RhX(dphos)(CO)], reasoning that the different *trans* influence and *trans* effect of the substituent would favour the formation of different isomers.

1.2.5 Electronic and Steric Effects in Phosphines

The electronic and steric properties of phosphine ligands have been found to dramatically influence the reactivity of their organometallic complexes. The

Chapter 1 10 Introduction

electronic properties of the ligand relates to the electronic character of the ligand-metal bond, *i.e.* to the extent of overlap of orbitals and amount of net charge transfer between ligand and metal. The relative importance of "electronic" and "steric" factors in the bonding between phosphines and metals, the division of into σ and π components, and the roles that these play in determining the physical and chemical properties of phosphine complexes were clearly described in classical reviews by Chatt and Williams, ⁴³ and Tolman. ⁴⁴

1.2.5.1 The Bonding of Phosphorus(III) to Transition Metals

In 1951 Chatt and Williams proposed that in metal phosphine complexes the σ -bond formed between the ligand lone pair and an empty metal orbital was reinforced by π -back bonding from the metal d orbitals to the phosphorus 3d orbitals (Figure 1.7).⁴³

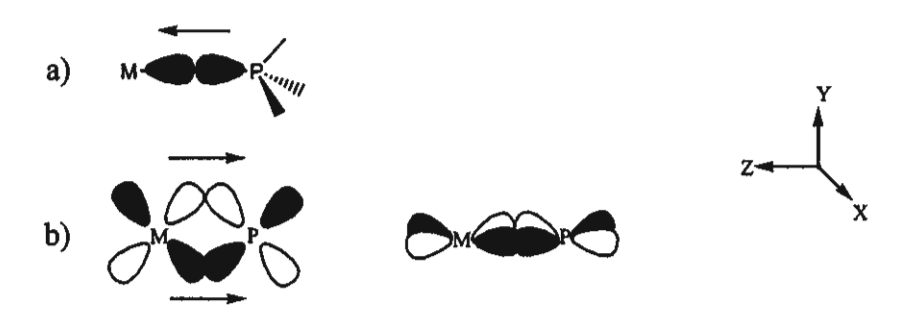


Figure 1.3 The classical view of the principal M-P bonding interactions in metal-phosphine complexes: a) P to M σ donation; b) π -backbonding from filled metal d_{XZ} and d_{YZ} orbitals to empty phosphorus $3d_{XZ}$ and $3d_{YZ}$ orbitals

The bonding in phosphine ligands, like that of carbonyls can be thought of as having two important components. The primary component is sigma donation of the phosphine lone pair to an empty orbital on the metal. The second component is backdonation from a filled metal orbital to an empty orbital on the phosphine ligand. This empty phosphorous orbital has been described as being either a d-orbital or an antibonding sigma orbital; current consensus is that the latter is more appropriate given the relatively high energy of a phosphorous d-orbital:

As electron-withdrawing (electronegative) groups are placed on the phosphorous atom, the σ -donating capacity of the phosphine ligand tends to decrease. At the same time, the energy of the π -acceptor (σ^*) on phosphorous is lowered in energy, providing an increase in backbonding ability. Therefore, phosphines can exhibit a range of sigma donor and π -acceptor capabilities, and the electronic properties of a metal center can be tuned by the substitution of electronically different but isosteric phosphines.

A rough ordering of the π -accepting or σ -donating capabilities of phosphines can be accomplished by synthesizing a series of complexes in which the only difference is the nature of the phosphine ligand. If these complexes contain a carbonyl ligand, then the CO stretching frequency can be used as an indicator of electron density at the metal (the lower the value of the CO stretching frequency, the greater

Introduction Chapter 1

the backbonding to the metal and thus the higher the electron density at the metal). Experiments such as this permit us to come up with the following empirical ordering:

1.2.5.2 Steric Effects in Phosphines

Phosphines are easy to synthesize and are excellent ligands for transition metals. As a consequence, the steric attributes of the phosphine ligand are easily controlled. This ability to control the bulk of the ligand permits one to tune the reactivity of the metal complex. For example, if the dissociation of a phosphine ligand is the first step in a reaction, the reaction can be accelerated by utilizing a larger phosphine ligand. Likewise, if dissociation is a problem, then a smaller phosphine can be used.

Studies of the steric properties of ligands centre on organometallic systems. The steric effect is a measure not merely of ligand size, but also of its spatial requirements in the coordination environment. The most popular method of evaluating ligand steric behaviour is to measure requirements the Tolman cone angle. 44-46 The cone angle concept was originally applied as a quantitative measurement of the steric requirements of phosphine ligands, but has since been extended to amines⁴⁷⁻⁴⁸ and other ligands. The cone angle (θ) is defined as the apex angle of a cylindrical cone, with origin 2.28Å from the centre of the phosphorus atom. whose sides just touch the van der Waals surfaces of the outermost atoms of the organic substituents (Figure 1.4). Tolman constructed Corey-Pauling-Koltun (CPK) space-filling models of various phosphines and measured their cone angles using a special jig and protractor. In cases where various conformations of the groups bound to phosphorus are possible, the groups were folded back to give the smallest possible cone angle while still maintaining a nominal three-fold symmetry axis.

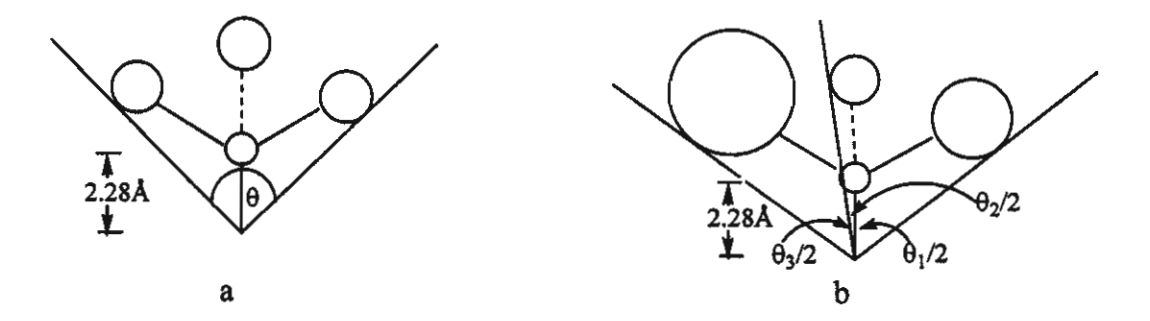


Figure 1.4 a) The geometrical definition of the cone angle b) The geometrical definition of the semicone angle

For unsymmetrical phosphines PRR'2 and PRR'R", Tolman suggested that an 'effective' cone angle can be obtained using the 'half-angles', or semicone angles, $\theta_i/2$, illustrated in Figure 1.4b. The effective cone angle is defined in terms of the average of the maximum half-angles (Equation 1.4).

$$\theta = \frac{2}{3} \sum_{i=1}^{3} \frac{\theta_i}{2}$$

Cone angles are based on a typical Ni-P bond length (2.28Å). The value of a ligand cone angle can be modified to take account of the transition metal involved by using other M-P bond lengths.

For chelating diphosphines, the cone angle at each phosphorus atom is defined as the angle between one M-P bond and the vector which bisects the P-M-P bite angle (β) plus the contributions of the non-bridging substituents on phosphorus (Figure 1.5).⁴⁹

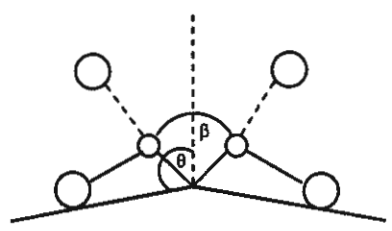


Figure 1.5 Ligand cone angle (θ) for chelating diphosphine. Note the dependence of cone angle upon the PMP bite angle (β).

The concept of the Tolman's cone angle as a measure for the steric bulk of monodentate phosphine and phosphite ligands has received widespread attention among chemists. However, the extension to bidentate ligands has been used less.

Cone angles for some common phosphine ligands are:

Phosphine Ligand Cone Angle Phosphine Ligand Cone Angle

| PH ₃ | 87° | PEt ₃ | 132° |
|------------------|------|----------------------|------|
| PF ₃ | 104° | PPh_3 | 145° |
| PMe ₃ | 118° | P(t-Bu) ₃ | 182° |

1.3 Introduction to Methanol Carbonylation

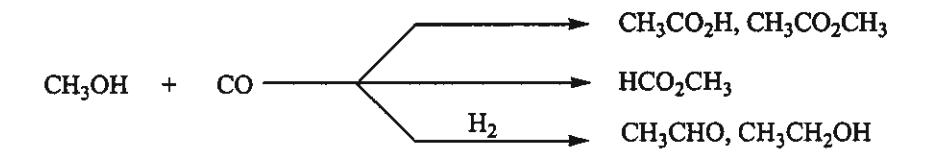
1.3.1 Methanol and Carbon Monoxide

Methanol is a versatile, readily available C₁ compound obtained from synthesis gas. The first methanol carbonylation process was developed by BASF using an iodide - promoted cobalt catalyst at high temperature (230 °C) and high pressure (600 atm) with selectivity of *ca.* 90% and is now considered to be only of historical interest. ⁵⁰⁻⁵¹ It is a large-scale industrial methanol production. At present, methanol still is produced almost exclusively from synthesis gas (a mixture of H₂, CO and some CO₂) in a gas-phase reaction over copper-based catalysts such as Cu/ZnO/Al₂O₃ or Cu/ZnO/Cr₂O₃ at temperatures ranging from 200 to 270°C and pressures from 50 to 100 bars, according to Equation 1.5.

$$CO + 2H_2$$
 — CH₃OH 1.5

The present methanol production capacity has been reported to be 21 million tons/years, while the actual demand is only in the range of 12 million tons/years.⁵⁰ This overcapacity is mainly due to the set-up of new plants, where surplus natural gas is available at a very low price.⁵² The ready supply as well as the low raw material costs will keep the price of methanol down in the near future. This will stimulate the demand of methanol and will help to introduce new methanol-based processes for motor fuels as well as for basic organic chemicals.⁵³

The present industrial uses of methanol include the production of formaldehyde, methyl esters, methylamines and methyl halides. In addition, methanol and its derivatives find an increasing interest as substrates for carbonylation and dehydration reactions, which are summarized in Scheme 1.1.



Scheme 1.1 Summary of industrial methanol conversion reactions

Some of these processes have already been used for the commercialization of acetic acid, acetic anhydride, or methyl formate. With methanol from cheap natural gas becoming available in the near future, these processes, although uneconomic today, might become industrially attractive.

Carbonylation catalysis encompasses a large and important area of chemistry. The majority of carbonylation reactions is carried out in homogeneous phase, because homogeneous catalysts generally give higher rates and selectivities than heterogeneous systems.

1.3.2 The Methanol Carbonylation

A major advance came in 1966 with the discovery of rhodium-iodide catalysts for the carbonylation of methanol by Monsanto, which led to the start-up of the first commercial unit in 1970. This is the second largest homogeneous catalytic industrial process with over 7 billion pounds of acetic acid produced each year using this technology.

The manufacture of acetic acid is one of the most important industrial processes with worldwide production capacity currently estimated at 7 million tons per annum. The main uses of acetic acid are in the production of vinyl acetate terephthalic acid. More than 50% of annual world acetic acid production is derived from the rhodium-catalyzed methanol carbonylation process and has thus been heralded as the most successful example of an industrial process utilizing a metal complex in solution (Equation 1.6).

CH₃OH + CO
$$\xrightarrow{\text{Rh, I}}$$
 CH₃COOH 1.6

The advantages of this process are low-pressure reaction conditions, low catalyst concentration and high product selectivity.

In 1970 Monsanto commercialized a rhodium carbonyl iodide catalyst that is commonly called the Monsanto Acetic Acid Process (developed in the late 60's by James Roth at the corporate research center in St. Louis). In the Monsanto process, methanol is combined catalytically with carbon monoxide to give acetic (ethnic) acid. This reaction is done in the presence of a catalyst. Forster did much of the original work. British Petroleum now runs this process.

In 1986 Monsanto sold the acetic acid plant and technology to British Petroleum, but it is still commonly referred to as the Monsanto Acetic Acid process. BP Chemicals who further developed the process and licensed it around the world.

In 1996, BP Chemicals announced a new catalytic process for the carbonylation of methanol to acetic acid named CativaTM; this process is based on a catalyst system composed of iridium complexes with ruthenium activators.⁵⁰

1.3.3 The Methanol Carbonylation Produces Acetic Acid

As known, acetic acid is an important industrial commodity chemical, with a world demand of about 6 million tons per year and many industrial uses. Novel acetic acid processes and catalysts have been introduced, commercialized, and improved continuously since the 1950s. The objective of the development of new acetic acid processes has been to reduce raw material consumption, energy requirements, and investment costs. At present, industrial processes for the production of acetic acid are dominated by methanol carbonylation and the oxidation of acetaldehyde.

Table 1.1 Industrial routes to acetic acid

| Method | Catalyst | Conditions | Yield |
|------------------------|---------------------------------|----------------------|-------|
| Methanol Carbonylation | Rhodium or Iridium complexes | 180-220 °C 30-40 bar | 99% |
| Acetaldehyde Oxidation | Manganese or cobalt acetate | 50-60 °C1 bar | 95% |

Group VIII transition metal complexes catalyze the carbonylation of methanol, especially by rhodium, iridium, cobalt, and nickel. 54-58

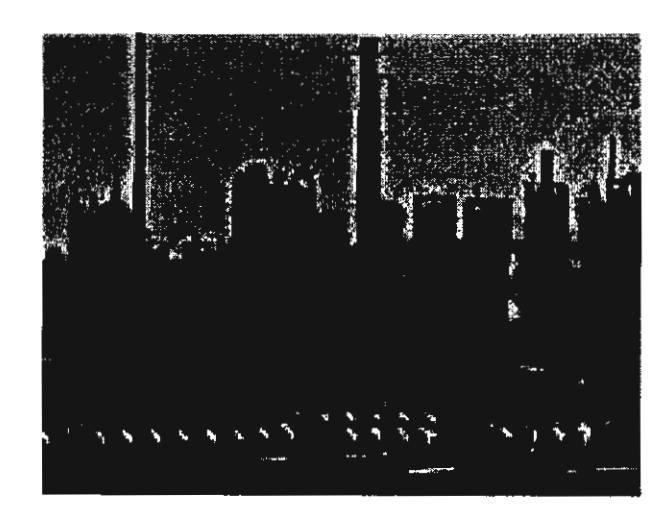
$$CH_3COOH + CH_3OH \longrightarrow CH_3COOCH_3 + H_2O$$
 1.7

All methanol carbonylation processes need iodine compounds as essential cocatalysts, the reaction proceeding *via* methyl iodide, which alkylates the transition metal involved. Apart from acetic acid, the carbonylation of methanol (Equation 1.6) gives also rise to the formation of methyl acetate, according to Equation 1.7. In some carbonylation processes (CativaTM), methyl acetate is also used as a solvent. The cobalt-catalyzed BASF process was introduced in the late 1950s, and the rhodiumbased Monsanto process followed in the early seventies. As it is evident from Table 2,⁵⁹⁻⁶¹ rhodium catalysts operate at very mild conditions and with very high selectivities, as compared to cobalt or nickel catalysts. It is therefore not surprising that most commercial plants now use the rhodium-based Monsanto process. Meanwhile, the worldwide capacity for acetic acid from methanol is well over 1,000,000 tons/years and is expected to increase further.⁶²

Table 1.2 Acetic acid production by carbonylation of methanol

| Catalyst | Temperature (°C) | Pressure (bar) | Selectivity (%) |
|--|------------------|----------------|-----------------|
| Rh ₂ O ₃ /HI | 175 | 1-15 | 99 |
| Co(OAc) ₂ /CoI ₂ | 250 | 680 | 90 |
| Ni(CO)4/MeI/LiOH | 180 | 70 | 84 |

Typical side reactions of the methanol carbonylation to acetic acid (Eq 1.6) are the formation of methyl acetate, methyl formate, dimethyl ether and the water-gas shift reaction, the formation of methyl acetate (Eq.1.7) being the most important one. These reactions are equilibria, which can be controlled by reaction conditions, catalyst metals, ligands, promoters, and solvents.



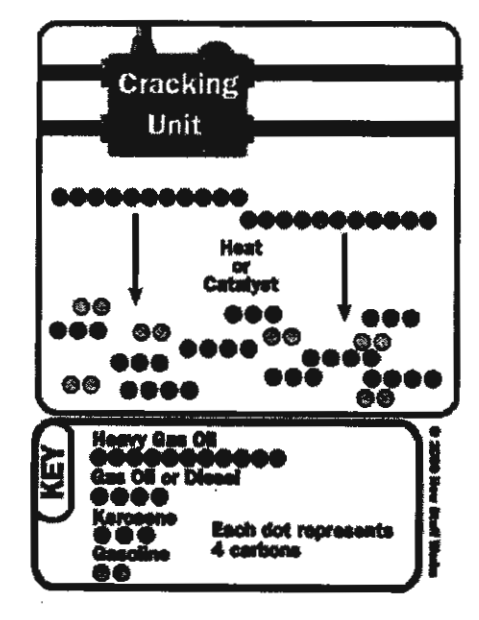


Figure 1.6 Oil refining: Catalysts for converting crude oil to gasoline

Quantum Mechanics Calculation: Asymmetric Phosphine for Methanol Carbonylation

16 Introduction

Chapter 1

1.4 Introduction to Homogeneous Catalysis by Transition Metal Phosphine Complex

Homogeneous catalysis provides an important application and fuels. Homogeneous catalysis, with advantages in selectivity, milder conditions for reactions, and economy in reagents, will become more important as resources diminish. As shown in Table 1.3 a number of industrial process use homogenous catalysts. 63-65

Table 1.3 Some processes catalysed homogeneously⁶⁴

| Reaction | 1990 Production ^a |
|-------------------------------|------------------------------|
| hydroformylation | 1818 |
| hydrocyanation (adiponitrile) | 420 |
| alkene polymerisation | 10000 |
| methanol carbonylation | 1164 |

a In thousands of metric tons

While the processes in Table 1.3 produce bulk commodities, stereospecific syntheses are beginning to have a major impact on the pharmaceutical industry to produce products such as *l*-dopa.⁶⁶⁻⁷⁰

1.4.1 Chelating Phosphines in Homogeneous Catalysis

The study of homogeneous catalysis by phosphine complexes began flourishing in the 1950s. It was spurred by Ziegler's discovery that the products of the reaction of triethylaluminium with certain complexes of zirconium or titanium were excellent catalysts for the polymerisation of ethene at ordinary temperatures and pressures.

The great strength of homogeneous catalysis and especially of that involving phosphine ligands, is the opportunity it affords to tailor ligands so as to enhance the reactivity and selectivity of the catalyst. Only a slight change in the ligand can effect considerable changes in selectivity. The reactions occur in homogeneous solution which facilitates the study of the mechanistic steps involved in the catalytic cycle and, by changing the phosphine and the metal, may allow the isolation of stable substances that are analogues of intermediates in the catalytic cycle. Although much progress has been made, many large-scale reactions used in the petrochemicals industry are still catalysed heterogeneously. The present thrust in homogeneous catalysis research is not only to increase reactivity and tailor the ligands to attempt to promote selectivity in the desired reaction, but also to render catalysts heterogeneous for convenience in use by attaching them to a surface, hopefully without loss of reactivity or selectivity. 71

Another reason for the success of phosphine ligands in homogeneous catalysis is that the ligands can be easily modified for a particular purpose. The immense amount of academic and industrial research over the past 25 years into factors that control the activity and selectivity of metal phosphines have been driven by the idea that rational design of homogeneous catalysts should be possible. A great variety of

Chapter 1 17 Introduction

phosphines have been made and these ligands can be fine tuned for catalysis through three main areas, as shown by Figure 1.7.

remote effects
$$\longrightarrow$$
 $M = metal centre$

$$R = substituent$$
stereoelectronics

Figure 1.7 Possible sites for modification of phosphorus(III) ligands

Factors such as steric and electronic properties, the ligand backbone and solubility can all be varied. Altering the steroelectronics of the R group, varying the bite angles, introducing chirality and introducing remote substituent effects (e.g. water-solubility to allow two phase catalysis) are all ways in which phosphine ligands can be tailored for catalysis. This is possible because the tertiary phosphine group is compatible with many other functional groups and their syntheses are generally straightforward. This means that ligand design is possible with tertiary phosphines to a degree that is unmatched by any other class of ligands used in catalysis at present.

This precise control of ligand behaviour is important because the activity and selectivity of catalytic processes is very sensitive to the structure of the ligand. The copolymerisation of carbon monoxide and ethene, for example, is catalysed by a palladium/diphosphine system.⁷² Very high activity is observed when the bridge, three carbon diphosphine contains a dppp e.g. bis(diphenylphosphino)propane). However, the system becomes virtually inactive when monodentate phosphines are used. Indeed, chelating diphosphines are favoured for many catalytic processes over their monodentate counterparts. hydroformylation, for example, rhodium-diphosphine systems were found to give an increased linear to branched ratio compared to rhodium-monophosphine analogues.⁵⁰ Casey et al. reported that diphosphine ligands with natural bite angles (i.e. the preferred chelation angles determined only by ligand backbone constraints and not by the metal valence angles) near 120° increase the selectivity for the formation of the linear aldehyde product in rhodium catalysed hydroformylation of 1-hexene.⁷³ Moreover, van Leeuwen showed that increasing the bite angles of bidentate diphosphines using xanthene-like backbones led to a regular increase in the regioselectivity of the hydroformylation of 1-octene for natural bite angles between 112 and 120°.74 The ligand backbone can also be used to introduce chirality for use in asymmetric catalysis. 75-76 Asymmetric catalysis involving organometallic species is undergoing rapid development and it is clear that phosphine ligands are central to this growth.

Phosphines have had extensive use in a range of complexes due to their ability to stabilise unusually high oxidation states of the late transition metals. They may be thought of as having high ligand field strengths, which render them compatible with ligands such as CO, hydride, saturated organic and alkyl/aryl groups, all of which are important in homogeneous catalysis.

Diphenylphosphines have found wide-ranging applications in coordination chemistry; most work to date has been concentrated on diphosphines with aryl substituents $^{77-81}$ rather than with alkyl substituents. 82 This is most likely a reflection of the greater availability and easier handling of aryldiphosphines rather than any intrinsic lack of interest since the high basicity of alkyldiphosphines makes them excellent ligands for metals in high and low oxidation states. A growing area of research involves species with biphenyl and binapthyl backbones. 83 Catalytic research in this area has focused on the design of ligands with C_2 -symmetry which have been proven to contribute significantly to high catalytic efficiencies and enantioselectivities. 84

1.5 References

- W.J. Hehre, *Practical Strategies for Electronic Structure Calculations*, University of California, USA, 1995.
- 2 E. Schrödinger, Ann. Physik, 1962, 79, 361.
- J.-P. Doucet and J. Weber, Computer-aided Molecular Design Theory and Applications, Academics Press, UK, 1997.
- 4 R.H. Boyd, J. Chem. Phys., 1968, 49, 2574.
- 5 M Born and J.R. Oppenheimer, Ann. Physik, 1927, 84, 457.
- 6 C.J.J. Roothaan, Rev. Mod. Phys., 1951, 23, 69.
- W.J. Hehre, L. Radom, P.v.R. Schleyer and J.A. Pople, Ab Initio Molecular Theory, Wiley, New York, 1986.
- 8 M. Planck, Ann. Physik., 1901, 4, 553.
- 9 a) A. Dedieu and A. Strich, *Inorg. Chem.*, 1979, 18, 2941.
- b) A. Dedieu, Inorg. Chem., 1981, 20, 2803.
- 10 A. Veilard, Chem. Rev., 1991, 91, 743.
- 11 a) N. Koga and K. Morokuma, Chem. Rev., 1991, 91, 823.
 - b) N. Koga and K. Morokuma, J. Am. Chem. Soc., 1985, 107, 7230.
- 12 K. Raghavachari, Annu. Rev. Phys. Chem., 1991, 42, 615.
- 13 S. Saebø and P. Pulay, Annu. Rev. Phys. Chem., 1993, 44, 213.
- W.J. Hedre, L.Radom, P.v.R Schleyer and J.A. People, Eds., *Ab initio Molecular Orbital Theory*, J. Wiley & Sons, New York, 1986.
- 15 P. Pulay and S. Saebø, *Theor. Chim. Acta.*, 1986, **69**, 357.
- 16 P. Pulay and S. Saebø, J. Chem. Phys., 1987, 86, 914.
- 17 M.J. Frisch, J.A. Pople and J.S. Binkley, J. Chem. Phys., 1984, 80, 3265.
- 18 N. Koga, J.O. Sin and K. Morokuma, J. Am. Chem. Soc., 1988, 110, 3417.
- 19 D.J. Musaev and K. Morokuma, *J. Organomet. Chem.*, 1995, **504**,93.
- J. Sadlej, Semi-empirical Methods of Quantum Chemistry, Ellis Horwood, Poland, 1985.
- 21 W. Thiel, Tetrahedron, 1988, 44, 7393.
- 22 M.J.S. Dewar and N.L. Sabelli, J. Chem. Phys., 1961, 34, 1232.
- 23 M.J.S. Dewar and W. Thiel, J. Am, Chem. Soc., 1977, 99, 4857.
- 24 M.J.S. Dewar and W. Thiel, J. Am, Chem. Soc., 1977, 99, 4907.
- 25 M.J.S. Dewar, E.G. Zoebisch, E.F. Healy and J.J.P. Stewart, *J. Am. Chem. Soc.*, 1985, 107, 3902.
- P. Hohenberg and W Kohn, in Homogeneous Electron Gas; *Phys. Rev.*, 1964, 134, 864.
- 27 a) C. Lee, W. Yang and R.G. Parr, Phys. Rev. B, 1988, 37, 785. b) A.D. Becke, J. Chem. Phys., 1993, 98, 5648.
- 28 see, T. Ziegler, Chem. Rev., 1991, 91, 651.
- 29 P. Margl, T. Ziegler and P.E. Blöchl, J. Am. Chem. Soc., 1995, 117, 12625.
- J.B. Foresman, Exploring Chemistry with Electronic Structure Methods, 2nd Eds., USA, 1996.
- 31 a) J.C. Slater, Phys. Rev., 1929, 34, 1293.
 - b) J.C. Slater, Phys. Rev., 1930, 36, 57.
 - c) J.C. Slater, Phys. Rev., 1951, 81, 385.
- 32 a) S.F. Boys, *Proc. Roy. Soc. Ser A.*, 1950, **200**, 542.
 - b) S.F. Boys and F. Bernardi, *Molec. Phys.*, 1970, 19, 558.

- J.F. Dobson, G. Vignale and M.P. Das, *Electronic Density Functional Theory-*Recent Progress and New Direction, Plenum, 1998.
- J. Chatt in *Homogeneous Catalysis with Metal Phosphine complexes*, Ed. L.H. Pignolet, Plenum Press, New York, 1983, 1.
- 35 R.B. King and P.N. Kapoor, J.Am. Chem.Soc., 1969, 91, 5191.
- 36 S.O. Grim, R.P. Molenda and R.L. Keiter, Chem. And Ind., 1970, 1378.
- 37 R.B. King, J. Bakos, C.D. Hoff and L. Marko, Inorg. Chem., 1979, 44, 3095.
- 38 A. Hessel and O. Stelzer, J. Org. Chem., 1997, 62, 2362.
- J.A.B. Van Doorn, N.B. Meijboom and R.L. Wife, Chem. Abstr., 1989, 110, 75803n; European. Pat., 286, 196, 1988.
- 40 K.V. Katti and R.G. Cavell, Organometallics, 1989, 18, 2147.
- 41 P.N. Kapoor, D.D. Pathak, G. gaur and M. Kutty, Inorg. Chim Act., 1986, 112, 153.
- 42 S.O. Grim, j.d. Gaudio, R.P. Molenda, C.A. Tolman and J.P. Jesson, J.Am.Chem. Soc., 1974, 96, 3146.
- 43 J. Chatt and A.A. Williams, J. Chem. Soc., 1951, 3061.
- 44 C.A. Tolman, Chem. Rev., 1977, 77, 313.
- 45 C.A. Tolman, J. Am. Chem. Soc., 1970, 92, 2956.
- 46 C.A. Tolman, W.C. Seidel and L.W. Gosser, J. Am. Chem. Soc., 1974, 96, 53.
- 47 A.L. Selingson and W.G. Trogler, J. Am. Chem. Soc., 1991, 113, 2520.
- 48 T.L. Brown and K.J. Lee, Coord. Chem. Rev., 1993, 128, 89.
- 49 C.P. Casey and G.T. Whiteker, *Isr. J. Chem.*, 1990, **30**, 299.
- 50 K. Kobayashi, Chem. Econ. Eng. Rev., 1984, 16(6), 32.
- 51 H. Itami, Chem. Econ. Eng. Rev., 1984, 16(4), 21.
- 52 K.Kobayashi, Chem. Econ. Eng. Rev., 1982, 14(4), 20.
- N. Yoneda, S. Kuzano, M. Yasui, P. Pujado and S. Wilcher, Applied Catalysis A: General, 2001, 221, 253.
- J. Falbe, Synthesen mit Kohlenmonoxid; Springer Verlag, Berlin, 1977.
- J. Falbe, Methodicum Chimicum, Georg Thieme Verlag, Stuttgart, 1975, 5.
- N.V. Kutepow and Himmele, *Ullmanns Encyclopädie der technischen Chemie*, 4th edition, Verlag Chemie, Weinheim, 1975, 9, 155.
- 57 D. Forster, Adv. Organomet. Chem., 1979, 17, 255.
- 58 F. Paulik and J.E.Roth, J. Chem. Soc., Chem. Commun., 1968, 1578.
- N. von Kutepow, W. Himmele, H. Hohenschutz, Chem. Ing. Techn., 1965, 37, 297.
- J. Gauthier-Lafave and R. Perron, Eur. Pat. Appl. 1981, 35458.
- 61 D. Forster and M. Singleton, J. Mol. Catal., 1982, 17, 299.
- 62 M.J. Howard, M.D. Jones, M.S. Roberts, S.A. Taylor, *Catal. Today*, 1993, 18, 325.
- J.D. Atwood, Inorganic and Organometallic Reaction Mechanisms., 2nd Edn, VCH Publishers(UK)Ltd., 1996, 180.
- a) G.W. Parshall, Homogeneous Catalysis, John Wiley and Sons, Inc., NY, 1980. b) G.W. Parshall and S.D. Ittel, Homogeneous Catalysis, 2nd Edn, John Wiley and Sons, Inc., NY, 1992.
- 65 C. Masters, Homogeneous Transition-Metal Catalysis: A Gentle Art, Chapman and Hall, 1980.
- 66 J. Chem. Ed., 1986, 63, is devoted to industrial applications of organometallic

- chemistry and catalysis. Specific manuscripts important to this topic are G.W. Parshall and R.E. Putsscher, general consideration, p189; B. Goodell, polymerization, p191; R.L. Pruett, hydroformylation, p196; C.A. Tolman, hydrocyanation, p.199; D. Forster and T.W. DeKleva, carbonylation of alcohols, p204; and W.S.Knowles, *l*-DOPA, p.222.
- 67 E. Muetterties and J. Stein, Chem. Rev., 1979, 79, 479.
- 68 C. Masters, Adv. Organomet. Chem., 1979, 17, 61.
- 69 M.D. Fryzuk and B. Bosnich, J. Am. Chem. Soc., 1978, 100, 5491.
- 70 K.E. Koenig and W.S. Knowles, J. Am. Chem. Soc., 1978, 100, 7561.
- see for example, F.R. Hartley and P.N. Vezey, Adv. Organomet. Chem., 1977, 15, 189.
- 72 a) E. Drent and P.H.M. Budzelaar, J. Organomet. Chem., 2000, 594, 2111.
- 73 C.P. Casey, G.T. Whiteker, M.G. Melvilee, L.M. Petrivich, J.A. Gavney, Jr. and D.R. Powell, J. Am. Chem. Soc., 1992, 114, 5535.
- M. Kranenburg, Y.E.M. van der Burgt, P.C.J. Kramer and P.W.N.M. van der Leeuwen, *Organometallics*, 1995, 14, 3081.
- 75 F. Agbossou, J.-F. Carpentier and A. Mortreux, Chem. Rev., 1995, 95, 2485.
- 76 M. Hodgson and D. Parker, J. Organomet. Chem., 1987, 325, C27.
- 77 G.J. Palenik, M. Matthew, W.L. Steffen and G. Beran, J. Chem. Soc. A., 1970, 1059.
- 78 W.L. Steffen and G.J. Palenik, *Inorg. Chem.*, 1976, 15, 2432.
- 79 R.O. Rosete, D.J. Cole-Hamilton and G. Wilkinson, *J. Chem. Soc., Dalton Trans.*, 1984, 2067.
- 60 G.P.C.M. Dekker, C.J. Elsevier anf K. Vrieze, Organometallics, 1992, 11, 1598.
- W.A. Hermann and C.W. Kohlpainter, Angew. Chem.; Int. Ed. Engl., 1993, 32, 1524.
- P. Palma-Ramirez, D.J. Cole-Hamilton, P. Pogorzelec and L. Campora, *Polyhedron*, 1990, **9**, 1107.
- a) J.M. Fox, X.H. Huang, A. Chieffi and S.L. Buchwald, J. Am. Chem. Soc., 2000, 122, 1360. b) M. Shaharuzzaman, J.B. Wilking, J.S. Chickos, C.N. Tam, R.A.G.D. Silva and T.A. Keiderling, Tet. Asym., 1998, 9, 1111.
- W.R. Moser and D.W. Slocum, Advances in Chemistry Series 230, Washington D.C., 1992





CHAPTER 2

LITURATURE REVIEW





Chapter 2 22 Literature Review

Chapter 2: Literature Review

A recent American Chemical Society Symposium volume on transition state modeling in catalysis illustrates its progress. This Symposium highlighted a significant development in the level of modeling that researchers are employing as they focus more and more on the highly quantum mechanical activated complexes of catalytic reactions. The complexity of catalytic processes had previously restricted full-scale computational efforts to the structure and binding of the reactive precursors.

To methanol carbonylation, the type of elementary steps has been examined separately in a number of theoretical and experimental studies.

In this chapter, a literature review involving quantum mechanics calculation about asymmetric phosphine for methanol carbonylation will be provide.

2.1 Quantum Mechanics Calculations: A Theoretical Study

The development of computational techniques such as the ab initio molecular orbital (MO) theory has made it possible to carry out calculations for organometallic compounds. Any theoretical studies have been published on elementary reactions of organometallic compounds including the methanol carbonylation process: oxidative addition, CO insertion, I ligand addition and reductive elimination. Studies of full catalytic cycles involving series of many elementary reactions, however, still remain as one of the theoretical challenges.

Improving manufacturing processes to make them more environmentally benign and to rationally design new materials will increasingly rely on computational chemistry. The rapid and efficient design of new materials, chemical intermediates, and product will be necessary to achieve the goals of greater energy efficiency and increased productivity while minimize environmental impact.¹¹

There have been a number of theoretical studies on methanol carbonylation process. They focused on an oxidative addition of organic molecules to unsaturated transition metal complexes which is a fundamental process in organometallic chemistry and plays a key role in many important catalytic reaction. ¹² An important example is the reaction of methyl iodide with cis- [M (CO)₂I₂] the rate determining step in the industrial carbonylation of methanol to acetic acid. ¹³⁻¹⁴ Ab initio transition structure have been located for nucleophilic attack by cis-[M(CO)₂I₂] (M=Rh, Ir) on MeI, and computed secondary α-deuterium kinetic isotope effects (KIEs) for the classical S_N2 mechanism are in excellent agreement with experiment for both Rh and Ir complexes. ¹⁵

Ligand steric and electronic effects play a key role in the determining organometallic reactivity trends and catalytic behavior. Gonsalvi and et. all showed that electronic and steric effects of ligands can combine to give rather surprising and dramatic effects on the rates of the key steps in catalytic cycle. ¹⁶ Unusually, the mixed P,S donor ligand, Ph₂P(CH₂)P(S)Ph₂ (dppms) is able to promote both oxidative addition, would normally be expected to inhibit CO insertion, but this is overcome by a steric of the dppms ligand.

Quantum mechanic calculations based on density functional theory (DFT) have been carried out on the migratory insertion process (equation 2.1). The first systematic study of migratory insertion process of direct relevance for the iridium-based carbonylation of methanol.¹⁷

$$[M(CO)_2I_3(CH_3)]^{-} \longrightarrow [M(CO)I_3(COCH_3)]^{-} 2.1$$
(M= Rh and IR)

The calculated free energy of activated ($\Delta G^{\#}$) are 27.7 kcal/mol (Ir) and 17.2 kcal/mol (Rh), in a good agreement with the experimental estimates at 30.6±1.0 Kcal/mol (Ir) and 19.3±0.5 Kcal/mol (Rh), respectively. The higher barrier for M=Ir is attributed to a relativistic stabilization of the Ir-CH₃ bond. It is indicated that enthalpy and entopic contributions to $\Delta G^{\#}$ can vary considerably. Especially, simulations based on ab initio molecular dynamics underlined that the reaction system might prefer to trad entropy for enthalpy in polar solutions by dissociating an Γ ligand for M=Ir.

A systematic study was also carried out on the general methyl migration reaction (equation 2.2).

$$[Ir(CO)_2I_2L(CH_3)]^{n-}$$
 \longrightarrow $[M(CO)I_2L(COCH_3)]^{n-}$ 2.2
(n= 0 and 1)
(L= CH₃OH, CH₃C(O)OH, CO, P(OCH₃)₃ SnI₃

Another ligand L or an empty coordinate site replaces the iodide ligand trans to methyl. The free energies of activation for the methyl migration following the order $P(OCH_3)_3 > CO > SnI_3^-$, none $>\Gamma > CH_3OH > CH_3C(O)OH$ with respect to the ligand L. This order is a first approximation determined by the ability of L to labilize the M-CH₃ bond *trans* to it. The order is further shaped by the ability of the π acceptors L=CO, $P(OCH_3)_3$ to stabilize the transition state and, in the case of L= none, by the relocation of an iodide ligand to the site trans to the migrating methyl group.

The potential energy profile of the full catalytic cycle of methanol carbonylation catalyzed by [Rh(CO)₂I₂] complex was explored computationally using a gradient-corrected density functional method. 18 The equilibrium structures of all isomers of the intermediate have involving the catalytic process have been calculated. The transition states of CH3I oxidative addition, the CO migratory insertion, and the CH3COI reductive elimination were also located. The rate determining step of the reaction, CH3I oxidative addition, was found to proceed via a backside S_N2 mechanism. The activation barrier of CO migratory insertion is calculated lower than of CH₃COI reductive elimination; this finding conforms the hypothesis that the unstable nature of complex [Rh(CH₃(CO)₂I₃] is mainly due to its fast decomposition into the acyl species. The trans conformers of the six coordinated intermediates [RhCH₃(CO)₂I₃] and [Rh(CH₃CO)(CO)₂I₃] are higher for the trans isomers than their cis conformer. The activation barrier of car migratory insertion into the Rh-CH₃ bond of [RhCH₃(CO)₂I₃] and CH₃COI reductive elimination from [Rh(CH₃CO)(CO)₂I₃] are higher to the trans-isomers than those of the corresponding cis isomers. Therefore, the lowest energy path is determined by the corresponding cid

Chapter 2 24 Literature Review

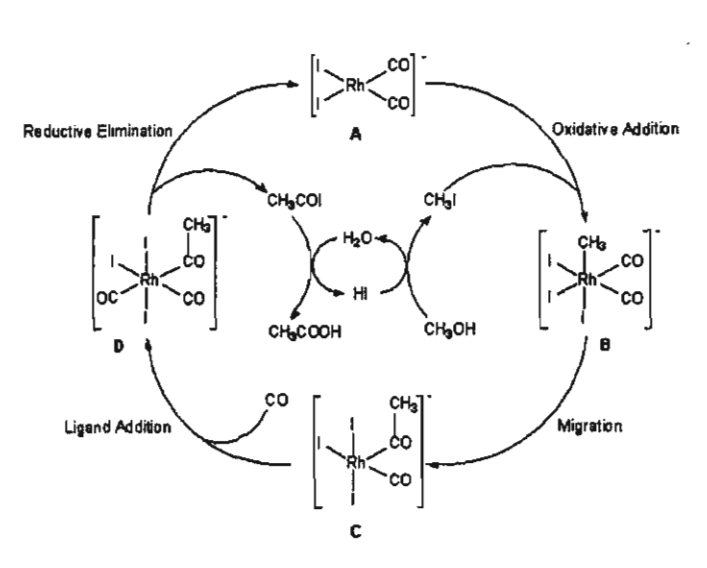
dicarbonyl species, which have to accessed by a ligand rearrangement. Solvent effects of the intermediates were calculated to increase from 6 fold to 5- fold to 4-fold coordinated complexes. While the solvent effects on the transition states are in general similar to those of the six-coordinated complexes, they affect oxidative addition and the reductive elimination steps in a crucial way.

A quantum mechanics (QM) and QM/MM (molecular mechanics) study on steric effect in the main steps of Rh catalyzed carbonylation reaction. 19 All considered system adopt a square-planar geometry prior to CH₃I oxidative addition. As regards the octahedral complexes after CH₃I oxidative addition, a comparison between the various models indicates the energy gain due to the CH₃I oxidative addition is reduce by steric pressure of the substitutions on the ligand. The substantially similar results obtained with the QM/MM and QM model indicate that electronic effects are not particularly relevant in the determining the energetic of oxidation addition. As regards the P,P-Ph octahedral complex, the geometry in which the CO group is trans to the CH₃ group, or trans to one of the P atoms, are of similar energy. A comparison between the various models indicates that the energy barrier of the CO insertion reaction is lowered by the presence of constituents on the chelating ligands. This effect is related to a relief of the steric pressure on the complex as the systems move from the six-coordinated octahedral geometry toward a five-coordinated squarepyramidal geometry. The energy barrier calculated for the P,S-Ph system is in rather good agreement with the experimental value, whereas that of the P.P-Ph system is somewhat under estimated. Inclusion of solvent effects with a continuum model leads to a slightly better agreement. The thermodynamic products adopt a square-pyramidal geometry with the COCH₃ group in the apical position.

2.2 Asymmetric Diphosphines in Methanol Carbonylation: An Experimental Study

More than twenty-five years after its discovery, the Monsanto catalyst [RhI2(CO)2]- is still a widely used commercial catalyst for the methanol carbonylation to acetic acid. ²⁰⁻²¹

The production of acetic acid by the Monsanto process is based on a rhodium catalyst and operates at a pressure of 30 to 60 bar and at temperatures of 150 to 200°C. The process gives selectivity of over 99 percent based on methanol. The catalytic cycle of this classic example of a homogeneous catalytic reaction consists of six steps (Scheme 2.1).²² The cycle includes several of the main reaction types known in organometallic chemistry,²³ such as oxidative addition, ligand migration, CO insertion, and reductive elimination. These types of elementary steps have been examined separately in a number of experimental and theoretical studies.²⁴⁻²⁷ Systematic studies including a detailed inspection of full catalytic cycles are much rarer.²⁸⁻²⁹ The catalytic cycle of methanol carbonylation was proposed²² on the base of selected data on structures of reactants and intermediates which have been identified by X-ray crystallography,³⁰ infrared and NMR spectroscopy.³¹



Scheme 2.1 Catalytic cycle of the rhodium-catalyzed methanol carbonylation

The reaction is first order with respect to [Rh] and [MeI] but independent of CO pressure and [MeOH]. It was suggested that the active species is [RhI₂(CO)₂] (A) and the first step is the oxidative addition of methyl iodide to form (B). This step is rate determining³² and (A) was the only detected species at that time by infrared spectroscopy at elevated temperature and pressure. The next step, migratory insertion is very rapid, so the intermediate (B) is extremely short-lived and only recently has it been detected using carefully chosen reaction conditions,³³ The reaction was carried out in neat iodomethane, which increased the steady state ratio of (B)/(A) and the low polarity solvent inhibited the rate of migratory insertion. Even so, the concentration of (B) was only 1% that of (A) but computer subtraction techniques allowed the $\nu(CO)$ for (B) to be observed. A 13C labelling experiment enabled an NMR spectrum of (B) to be recorded. Both the infrared and NMR spectroscopy suggested a cis, fac structure for B). The activation parameters for the oxidative addition show a large negative entropy and small positive enthalpy,34 that indicates an S_N2 mechanism for the oxidative addition. The activation parameters are similar to those for the overall methanol carbonylation cycle.³⁵ The extremely short lifetime and low concentration of (B) minimizes by-product formation (e.g. of methane) and thus accounts for the high selectivity of the process.³⁶

Migratory insertion results in the rhodium-acetyl complex (C), which can decomposed by loss of methyl iodide but addition of CO leads to the dicarbonyl (D) which reductively eliminates acetyl iodide to regenerate (A) thus completing the catalytic cycle. The acetyl iodide is hydrolyzed to form acetic acid and hydrogen iodide. Methanol reacts with the hydrogen iodide to produce water and regenerate methyl iodide.

The basic idea was that ligands, which increase the electron density at the metal, should promote oxidative addition and by sequence the overall rate of production. To modify this catalyst and increase its activity by introducing electron-donating ligands have been hampered by the instability of many complexes of such ligands under the harsh reaction conditions required for carbonylation. To this purpose, in the last year several other Rh compound gas been synthesized and have been demonstrated to be active catalysts of comparable or better performances compared to the original Monsanto catalyst. One of the most important classes is

based on Rh complexes containing simple phosphines such as PEt₃ or biphosphine ligand of the type PPh₂-CH₂-PPh₂.

Recent reports have identified a number of a mixed-donor ligands, which promote carbonylation under mild conditions (typically<130°C and <20 bar).³⁷⁻³⁹ However, these mild conditions are not well suited to commercial operation where high absolute reaction rates are required and engineering constraints favor high temperatures and therefore higher pressures. One report has stated that the use of the diphosphinesulfide Ph₂PCH₂P(S)Ph₂ (dppms) as a promoter for rhodium catalyzed methanol carbonylation allows a surprisingly substantial rate increase under industrially feasible conditions. At 185°C, 30 atm CO, the rate increased eight times higher than [RhI₂(CO)₂]⁻ (for commercial viability, the conditions under which the catalyst operates are crucial).

For commercial viability, the conditions under which the catalyst operates are crucial. The mild conditions used for Wegman's and Cavell's catalysts are not suited to commercial operation because high absolute reaction rates are required and engineering constants favor higher temperatures and pressures and under industrial process conditions, the catalysts developed by Cavell and Wegman afforded little rate increase over the ligand-free catalyst (Table 2.1). The conditions employed are very different to those used by Wegman and Cavell and the high temperatures and pressure are probably not the conditions at which these catalysts perform optimally.

Table 2.1 Relative rates of rhodium catalysts for methanol carbonylation^a screened by Baker *et al.*⁴³

| Ligand | Rate/mol ⁻¹ h ⁻¹ | | |
|--|--|--|--|
| - | 2.3 | | |
| Ph ₂ PCH ₂ P(S)Ph ₂ b | 19.6 | | |
| PPh ₃ | 2.6 | | |
| Ph ₂ PCH ₂ CH ₂ P(O)Ph ₂ | 2.7 | | |
| Ph ₂ PN(Ph)P(S)Ph ₂ | 3.5 | | |

a conditions used: 185 °C, 70 atm. A ligand: rhodium ratio of 4: 1 was used unless otherwise stated

b Ligand: rhodium ratio 1:1

The complex 2A was fully characterized and an X-ray crystal structure shows the phosphorus lies trans to the chloride. During the carbonylation, the only rhodium-carbonyl species observed by infrared spectroscopy was the chelated complex 2B. The $\nu(CO)$ of 2B suggests that the rhodium is more electron-rich than in $[RhI_2(CO)_2]^-$ and this may contribute to the higher overall rate of carbonylation. The catalytic cycle

was studied by infrared and ³¹P{¹H} NMR spectroscopies; there was no evidence of the ligand partially dissociating during the catalytic cycle. Kinetic studies on a model system at room temperature show the rate of oxidative addition is much higher than for [RhI₂(CO)₂], and migratory insertion is also rapid.

Scheme 2.2 The methanol carbonylation catalyzed by Rh[Ph₂PCH₂P(S)Ph₂](CO)I

The dppms ligand gives rapid oxidative addition and it also promotes the subsequent CO insertion step (by a factor of ca.3000 compared with Ph2PCH2CH2PPh2(dppe)). The fact that both oxidative addition and CO migratory insertion steps are accelerated with the latter ligand was quite unexpected, and it was hypothesized that the steric requirements of the steric requirement of the PPh2-CH2-P(S)-Ph2 ligand destabilized the octahedral intermediate, which would undergo migratory insertion to release such steric pressure.

The new CativaTM process uses an iridium-iodide catalyst and is even more efficient than rhodium system that it has begun to replace.⁴⁴ In contrast to the Monsanto process, the CativaTM process is easily poisoned by metals like iron and nickel, which inhibit the iodide loss step in the carbonylation cycle

However, the rhodium-iodide catalyzed process gives acetic acid in better than 99% selectivity and the mechanism has been studied. Even so, the development of catalysts with higher selectivity is one of the goals of current research with the emphasis on ligands that are electronically asymmetric. 16, 39,44, 46-48

Pringle *et al.* reported that rhodium complexes of unsymmetrical ethylene diphosphine ligands are more efficient catalysts than the symmetrical dppe analogues for methanol carbonylation and longer-lived than any other reported ligand-modified catalysts under industrial conditions.⁴⁹⁻⁵² The catalysts were prepared by addition of diphosphines to [Rh(CO)₂Cl]₂ in methanol (Scheme 2.3).

 $Ar = 4 - C_6H_4OMe \text{ or } 3.5 - C_6H_3F_2 \text{ or } 3.4.5 - C_6H_2F_3$

Scheme 2.3 Synthesis of rhodium complexes with asymmetrical phosphine ligands

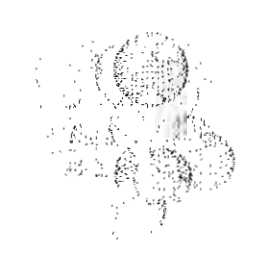
In each case the conversion of methanol was greater than 98%, and the selectivity for acetic acid was greater than 99%; however, the carbonylation rates are lower for these diphosphine complexes than for the [Rh(CO)₂I₂] catalyst. The following observations suggest that the catalyst is indeed a diphosphine-rhodium complex throughout the catalytic reaction and not [Rh(CO)₂I₂]. Infrared spectra obtained in situ during catalysis with Ph₂PCH₂CH₂P(3,4,5-C₆H₂F₃)₂ showed the absence of the intense v(CO) bands of $[Rh(CO)_2I_2]^2$ at 2059 and 1988 cm⁻¹. At the end of the catalytic reaction, ³¹P NMR and IR spectra showed the presence of a mixture of carbonyl diphosphine rhodium(III) complexes. The product Rh[Ph₂PCH₂CH₂P(3,4,5-C₆H₂F₃)₂](CO)I₃ was isolated from the reaction mixture, using the catalyst Rh[Ph₂PCH₂CH₂P(3,4,5-C₆H₂F₃)₂](CO)Cl.⁴⁹ The rate of catalysis is constant throughout a catalytic run and, after consumption of the entire methanol, a second aliquot of methanol was injected, the rate observed was the same as in the first run. This final observation not only confirms the integrity of the catalyst, but also shows its longevity to be greater than any previous rhodium-phosphine catalyst under these conditions, since every diphosphine complex executes over 500 turnovers without noticeable diminution of activity. The rhodium-diphosphine catalysts also resemble the iridium Cativa catalyst. The amount of propionic acid reported (formed during the water-gas shift reaction) for these diphosphine catalysts is significantly less than that with [Rh(CO)₂I₂] as catalyst under the same conditions.

2.3 References

- L. Parrill and M.R. Reddy, Rational Drug Design, Amarican Chemical Soc., New York, 1999.
- T. Matsubara, N. Koga, Y. Ding, D.G. Musaev and K. Morokuma, Organometallics, 1997, 16, 1065.
- 3 K. Kitaura, S. Obara, K. Morokoma, J. Am. Chem. Soc., 1981, 103, 2891.
- 4 S. Obara, K. Kitaura, K. Morokoma, J. Am. Chem. Soc., 1984, 106, 7482.
- 5 P.Hays, J. Am. Chem. Soc., 1987, 109, 705.
- 6 A.L. Sargent, M.B. Hall, *Inorg. Chem.*, 1992, 31, 317.
- 7 N. Koya, K. Morokoma, J. Phys. Chem., 1990, 94, 5454.
- 8 J.J. Low, W.A. Goddard, J. Am. Chem. Soc., 1984, 106, 8231.
- 9 A. Dedieu, *Inorg. Chem.*, 1981, 20, 2803.
- S. Sakaki, K. Kitaura, K. Morokoma, K. Ohkubo, J. Am. Chem. Soc., 1983, 105, 2280.
- D.G. Truhlar and K. Morokoma, *Transition State Modeling for Catalysis*, Amarican Chemical Soc., Washington, DC, 1999.
- P. Collman, L.S. Hegedus, J.R. Norton, R.G.Finke, *Principles and Applications of Organotransition Metal Chemictry*, University science Books: Mill Valley, CA, 1987.
- 13 D. Foster, Adv. Organomet. Chem., 1979. 17, 255.
- 14 A Haynes, B.E. Mann, G.E. Morris, P.M. Maitlis, *J. Am. Chem. Soc.*, 1993, 115, 4093.
- 15 T.R. Griffin, D.B. Cook, A. Haynes, J.M. Pearson, D. Monti, and G.E. Morris, J. Am. Chem. Soc., 1996, 118, 3029.
- 16 L. Gonsalvi, H. Adams, G.J. Sunley, E. Ditzel, and A. Haynes, J. Am. Chem. Soc., 1999, 121, 11233.
- 17 M. Cheong, R. Schmid and T. Ziegler, Organometallics, 2000, 19, 1973.
- 18 E.A. Ivanova, P. Gisdakis, V.A. Nasluzov, A.I. Rubailo and N. Rosch, Organometallics, 2001, 20, 1161.
- 19 L. Cavallo and M. Sola, J. Am. Chem. Soc., 2001, 123, 12294.
- a) M.J. Howard, M.D. Jones, M.S. Roberts and S.A. Taylor, *Catalysis Today*, 1993, 18, 325.
- M. Gauss, A. Seidel, P. Torrence and P. Heymans, in Applied Homogeneous Catalysis with Organometallic Compounds, ed. B. Cornils and W.A. Herrmann, VCH, New York, 1996.
- B.C. Gates, Catalytic Chemistry, Wiley: New York 1992.
- 23 N. Koga and K. Morokuma, J. Am. Chem. Soc., 1993, 115, 6883.
- 24 S. Sakaki, Y. Ujino, M. Sugimoto, Bull. Chem. Soc. Jpn., 1996, 69, 3047.
- 25 S.Sakaki, M. Ieki, J. Am. Chem. Soc., 1993, 115, 2373.
- 26 K. Albert, P. Gisdakis, R. Rösch, Organometallics, 1998, 17, 1608.
- T. Matsubara, N. Koga, Y. Ding, D.G. Musaev and K. Morokuma, Organometallics, 1997, 16, 1065.
- 28 A. Dedieu, Inorg. Chem., 1980, 19, 375.
- 29 P. Margl, T. Ziegler and P.E. Blöchl, J. Am. Chem. Soc., 1996, 118, 5412.
- F. Paulik and J.E. Roth, J. Chem. Soc., Chem. Commun., 1968, 1578.
- M.Bassetti, D. Monti, A. Haynes, J.M. Pearson, I.A. Stanbridge and P.M. Maitlis, Gaz. Chim. Ital., 1992, 122, 391.
- 32 D. Forster, J. Am. Chem. Soc., 1976, 98, 846.
- 33 M.F. Ernest and D.M. Roddick, Inorg. Chem., 1989, 28, 1624.

34 A. Haynes, B.E. Mann, G.E. Morris and P.M.Maitlis, J. Am. Chem. Soc., 1991, 113, 8567.

- 35 T.W. Dekleva and D. Forster, Adv. Catal., 1986, 34, 81.
- 36 D. Forster, *The Chemist*, 1981, 7.
- 37 R.W. Wegman, A.G. Abatjoglou and A.M. Harrison, J. Chem. Soc., Chem. Commun., 1987, 1891.
- 38 US Patent 46070570 to UCC (1987)).
- 39 PCT Patent Application WO 92/04118 to R.G. Cavell (1992).
- 40 M.J. Baker, M. F. Giles, A.G. Orpen, M.J. Taylor and R.J. Watt, J. Chem. Soc., Chem. Commun., 1995, 197.
- 41 K.G. Molly and R.W. Wegman, Organometallics, 1989, 8, 2883.
- 42 R.W. Wegman and D.J. Schreck, Chem. Abstr., 1991, 115,1845511c.
- 43 M.J. Baker, M.G. Giles, A.G. orpen, J. Taylor and R.J. Watt, J. Chem. Soc, Chem. Commun, 1995, 197.
- 44 a) Catava refs, Chem. and Ind., 1996, 483. b) BP patent ref, J.M. Pearson, A. Haynes, G.E. Morris, G.J. Sunley and P.M. Maitlis, J. Chem. Soc., Chem. Commun., 1995, 1045.
- 45 C.A. Carraz, D.D. Ellis, E.J. Ditzell, A.G. Orpen, P.G. Pringle and G.J. Sunley, J. Chem. Soc., Chem. Commun., 2000, 1277.
- d) P.M. Maitlis, A. Haynes, G.J. Sunley and M.J. Howard, J. Chem. Soc., Dalton Trans., 1996, 2187.
- 47 L.A. van der Veen, P.K. Keeven, P.C.J. Kamer, and P.W.N.M. van Leeuwen, J. Chem. Soc., Dalton Trans., 2000, 2105.
- 48 M.J. Baker, Rhodium Catalysed Methanol Carbonylation Promoted by Phosphine Ligands Part VI, BP Chemical, Hull, 1996.
- 49 C.P. Casey, E.L. Paulsen, E.W. Beuttenmueller, B.R. Proft, B.A Matter and D.R. Powell, J. Am. Chem. Soc., 1999, 121, 63 and references therein.
- 50 H. Brunner and A. Stumpf, *J. Organomet. Chem.*, 1993, 459, 139.
- 51 P. N Kapoor, D. Pathak, G. Gaur and M Kutty, *J. Organomet. Chem.*, 1984, 276, 167.
- 52 M.J.Howard, G.J. Sunley, A.D. Poole, R.J. Watt and B.K. Sharma, Stud. Surf. Sci. Catal., 1999, 121, 61.

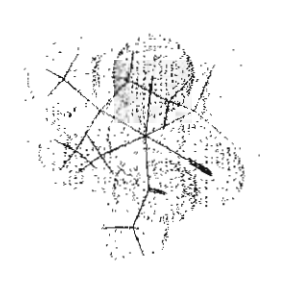




CHAPTER 3

SCOPE, AIMS AND METHODOLOGY





Chapter 3: Scope, Aims and Methodology

Methanol carbonylation with the original Monsanto catalyst has been studied in detail not only from an experimental but also from a theoretical point of view. In contrast, the same reaction promoted from phosphine-based ligands has been subject of detailed experimental research, but not from a theoretical point of view. This is despite the potential of molecular modeling to contribute to clarify the role of steric and electronic properties of different ligands in the determining the relative rate of the most important steps of catalytic cycle, i.e. the oxidative addition and CO migratory insertion. With the aim of filling this gap, here I present pure quantum mechanics, QM and sometimes combined a quantum mechanics and molecular mechanics calculations on some aspects of the cycle.

3.1 Scope and Aims

The basic idea was that ligands which increase the electron density at the metal should promote oxidative addition, ¹⁻² and by consequence the overall rate of the production. To this purpose, the scope and aim of this work are:

1. To evaluate and investigate the basic electronic features of asymmetric diphosphine ligand $F_2PCH_2CH_2PMe_2$ or 1.1. We hope this asymmetric diphosphine ligand is a promoter for methanol carbonylation catalysis. Such a ligand can be tuned to mimic the electronic properties by varying the constituents on one phosphorus i.e. make a 'strong-weak' ligand with one strong σ -donor (and poor π -acceptor) and one weaker σ -donor (and stronger π -acceptor). Theoretical methods are employed in this work.

$$C_3$$
 P_2
 P_1
 P_1
 P_2

Figure 3.1 A ligand 1.1

2. To evaluate asymmetric diphosphine rhodium complexes including a rhodium complex cation. Because of asymmetric ligand, 1.1 has a chiral center with electron withdrawing group and electron donating group. This would be the reason that the different trans-influence and trans effect of complex type "Rh (L) L' (1.1)" would favor the formation of different isomers as shown in Figure 3.2.

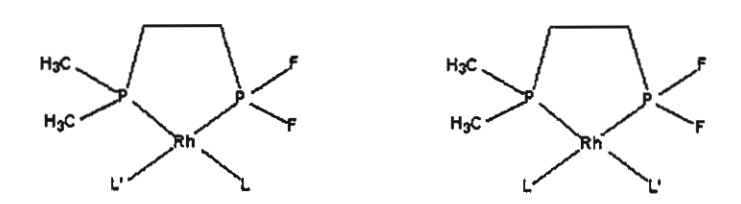
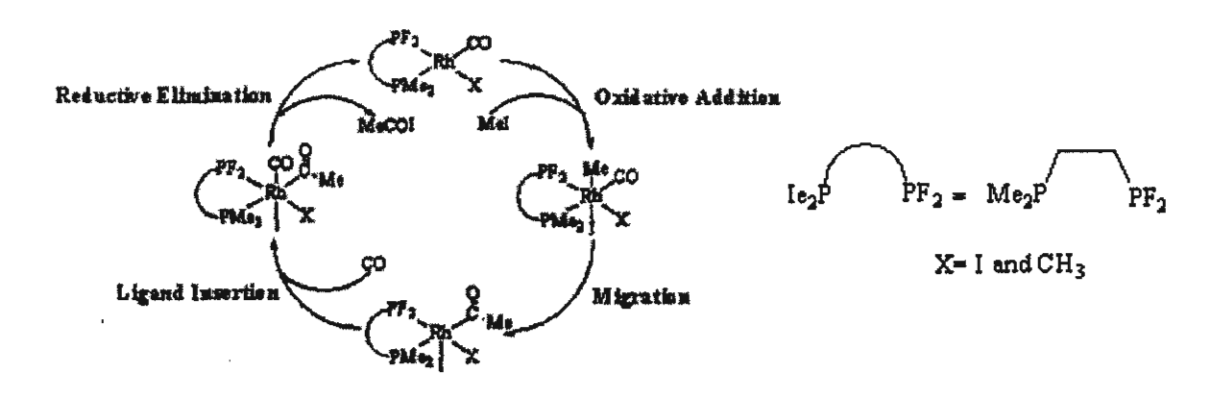


Figure 3.2 Proposed the formation of different rhodium isomers

- 3. To find the most stable asymmetric diphosphine rhodium isomer for using as starting isomer for methanol carbonylation cycle.
- 4. To evaluate the proposed cycle (Scheme 3.1). In this work, I am interested in the behavior of other types of complexes stabilized by asymmetrical ligands. The density functional theory is applied to four separate reactions of the methanol carbonylation cycle. Actually, only the outer cycle, which involves the organometallic compounds, is of interest in the present work; the purely organic steps, namely, the formation of CH₃I from methanol and the hydrolysis of CH₃COI to acetic acid, will not be considered in the following.



Scheme 3.1 Proposed catalytic cycle for methanol carbonylation in rhodium complexes.

5. To compare the electronic properties of rhodium asymmetric diphosphine complexes. This is to study their coordination properties and to exploit their catalytic potential for the carbonylation of methanol.

From a comparison between the results obtained with different ligands and with different methodologies, we hope to contribute to the rationalization of the experimental results and, possibly, to furnish ideas which might be used to design new and better ligands.

3.2 Methodology

3.2.1 Designed Structures.

The designed structures under this study are an asymmetric diphosphine ligand $F_2PCH_2CH_2PMe_2$ 1.1, a cation 1.2 and complexes 1.3, 1.4, 1.5 and 1.6. The complexes have square planar geometry at rhodium. Isomeric complexes 1.3 and 1.4 contain CO and Γ . An isomer 1.3 has CO trans to PMe₂ moiety of the ligand; this arrangement is reversed in 1.4. CO and I ligate isomeric complexes 1.5 and 1.6. They differ from complexes 1.3 and 1.4 only in that a Me group replaces the Γ ligands of 1.3 and 1.4. The structures are shown in Figure 3.3.

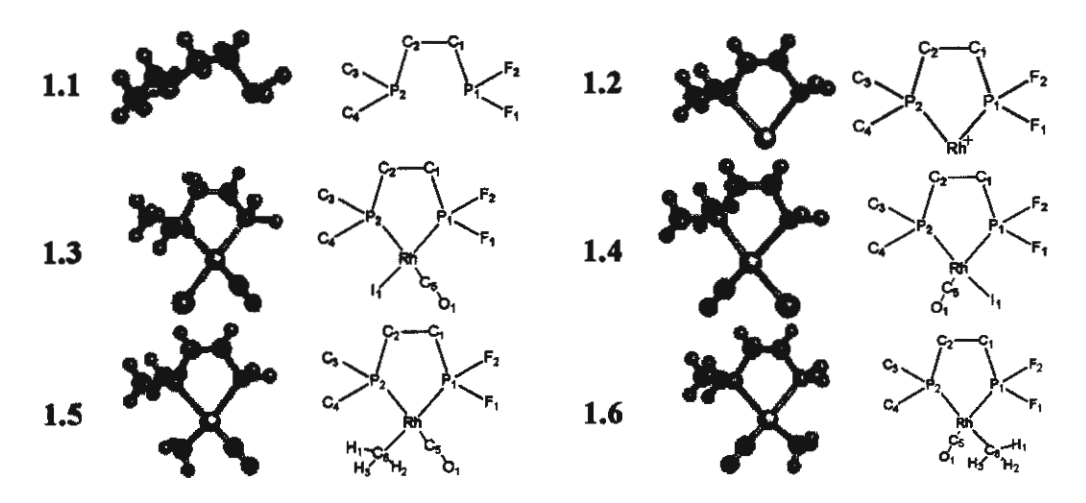


Figure 3.3 Designed ligand 1.1, cation 1.2, and complexes 1.3, 1.4, 1.5 and 1.6

3.2.2 Computational Methodology

The initial structure geometries for each molecule are constructed at the UFF level by using Ceruis² program.³ The "Drawing tool" menu is employed. A two-dimensional (2D) representation of a molecule is draw first, and then uses the Model Builder to generate a three-dimensional (3D) structure. However, to calculate the properties of a molecule, one needs to generate a well-defined structure. So, the geometry optimizations are started from an idealized symmetric geometry with chemically equivalent bonds and angles assigned to the corresponding values from International Tables for Crystallography (ITC).⁴

After the full optimization with Cerius², all optimized structures are transferred and then generated the input Gaussain format by the GaussView program.⁵ This program is the graphic user interface designed to help to prepare input for submission to Gausian 98 and to examine graphically the out put that Gausian produces.⁶ All structures will use a single point energy calculation to check out properties. All *ab initio* calculations are using a minimal basis set (3-21G)⁷⁻¹⁰ Then, in order to determine suitable approach, the performing needs the full optimization at Hartree-Fock (HF) level: HF/3-21G and density functional theory (DFT) level B3LYP/LANL2DZ. These optimized geometries are compared to those similar structures and UFF calculation.

The Gaussain series of Program¹¹, the software tools for calculation are based on semi-empirical information, ¹²⁻¹⁴ Hatree-Fock and Density Functional Theory.¹⁵ The geometries of all of intermediate in this work were fully optimized. The Cs symmetry was imposed for all complexes.

The stationary point found by a geometry optimization. As we noted, geometry optimizations converge to a structure on the potential energy surface where the forces on the system are essentially zero. Based on the best level, the molecular orbitals yielded from these quantum mechanics calculation were generated using GaussView program. The molecular orbital can also viewed by this program as well as optimized molecular molecular structures, electron density surfaces from computed

density, animation of the normal modes corresponding to vibrational frequencies and IR and Raman spectra.

3.3 Apparatus

The nature of his work is calculation by using the best and rapid computer as well as the best program suit.

3.3.1 High Performance Computer

3.3.1.1 Silicon Graphic Computer¹⁶

3.3.2 Softwares

- 3.3.2.1 Cerius² Program²
- 3.3.2.2 Gauss View³
- 3.3.2.3 Molden¹⁷
- 3.3.2.4 HyperChem¹⁸

3.4 References

- 1 M.J. Howard, M.D. Jones, M.S. Roberts and S.A. Taylor, *Catalysis Today*, 1993, 18, 325.
- M. Gauss, A. Seidel, P. Torrence and P. Heymans, in *Applied Homogeneous Catalysis with Organometallic Compounds*, ed. B. Cornils and W.A. Herrmann, VCH, New York, 1996.
- 3 Cerius² Version 2.5, Molecular Simulations, St. John Innovation Centre, Cowley Road, Cambridge, CB4 4WS, UK.
- 4 International Tables for Crystallography, Vol. C, 1992, Kluwer, Dordrecht.
- 5 Gauss View Version 2.0, Gaussian Inc., Pittsburgh, 1998.
- 6 A.B. Neilson and A.J. Holder, *GaussView's User Giude*, Gaussian Inc., Pittsburgh, 1998.
- 7 A.D. Becke, J. Chem. Phys., 1993, 98, 5648.
- 8 J.S. Binkley, J.A. Pople and W. Hehre, J.Am. Chem. Soc., 1980, 102, 939.
- 9 M.S. Gordon, J.S. Binkley, J.A. Pople and W. Hehre, J.Am. Chem.Soc., 1982, 104, 2797.
- 10 K.D. Dobbs and W. Hehre, J. Comput. Chem., 1987, 8, 880.
- M.J. Frisch, A.E. Frisch and J.B. Foresman, Gaussain 98 User's Reference, Gaussian Inc., Pittsburgh, 1999.
- 12 A.K. Rappé, C.J. Casewit, K.S. Colwell, W.A. Goddard III and W.M. Skiff, J. Am. Chem. Soc., 1992, 114, 10024.
- 13 N.L. Allinger and Y.H. Yuh, QCPE, 1980, 395.
- 14 A.K. Rappé, K.S. Colwell and C.J. Casewit, *Inorg. Chem.*, 1993, 32, 3438.
- see, T. Ziegler, Chem. Rev., 1991, 91, 651.
- 16 SGI O², Silicon Graphic Inc., USA.
- 17 Molden Version 2, Molden Inc., Netherland.
- 18 Hyperchem6 Professional, Version 6.0, Hypercube, Inc., USA.





CHAPTER 4

RESULTS AND DISCUSSION-1





Chapter 4: Results and Discussion-1 1.5 for Methanol Carbonylation

As stated in Chapter 3, actually only the outer cycle which involves the organometallic compounds is of interest in this work. The purely organic steps namely, the formation of CH₃I from methanol and the hydrolysis of CH₃COI to acetic acid, will not be considered in the following.

To follow this object, the calculation is divided into three steps. The first is to find the best calculation type for such these structures. This step is to apply a different calculation types to the representative structures to find the appropriate method to use as a tool for the following calculation. Later is to find the most stable structure. There are four organometallic rhodium complexes which are isomerical in this work. The aim of this step is to find the most stable structure to do calculation for the next step. The final step is to do full optimization methanol carbonylation cycle.

After find the most stable isomer, the outer methanol carbonylation cycle is explored. This process made up of 4 separate stoichiometric reactions.

4.1 To Find the Best Calculation Type for Such These Structures.

Because of an asymmetric bidentate rhodium complexes. It must be careful to choose the appropriate and the best tool for these such complexes. To do so, rhodium complexes 1.5 and 1.6 are chosen as the representative of these complexes and then did a full optimization. A various types of calculation are selected to find the best calculation method. Hartree-Fock with 3-21G and LANL2DZ level are applied as well as density functional theory with 3-21G and LANL2DZ. The structures are shown in Figure 4.1.

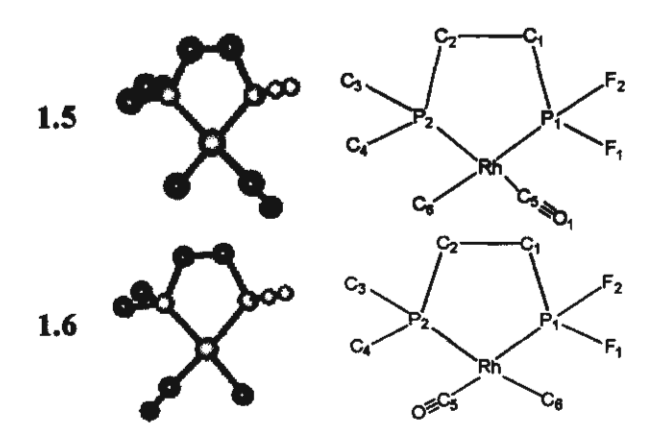


Figure 4.1 The structures of complexes 1.5 and 1.6. Hydrogen atoms are omitted for clarity.

The four different method optimized parameters of 1.5 and 1.6 are compared with the data from International Table for Crystallography (ITC)¹ is shown in Table 4.1.

Table 4.1 Comparison of computed rhodium complexes 1.5 and 1.6 at different levels of theory: HF/3-21G, HF/LANL2DZ, DFT/3-21G, DFT/LANL2DZ, and typical dimensions.

| | 1.5 | | | 1.6 | | | | | |
|-------------------|--------------|----------------|---------------|-----------------|--------------|----------------|---------------|-----------------|-------------------|
| Parameter | HF/ 3-21G | HF/ LANL2DZ | DFT/ 3-21G | DFT/ LANL2DZ | HF/ 3-21G | HF/ LANL2DZ | DFT/ 3-21G | DFT/ LANL2DZ | ITC |
| P1-F ⁴ | 1.851 | 1.684 | 1.665 | 1.740 | 1.622 | 1.662 | 1.682 | 1.732 | |
| P2-Me | 1.874 | 1.868 | 1.886 | 1.882 | 1.880 | 1.872 | 1.872 | 1.887 | |
| Rh-P1 | 2.425 | 2.437 | 2.312 | 2.357 | 2.560 | 2.441 | 2.566 | 2.507 | 2.41 ^b |
| Rh-P2 | 2.479 | 2.498 | 2.412 | 2.456 | 2.361 | 2.286 | 2.428 | 2.348 | 2.33° |
| Rh-C6 | 2.136 | 2.119 | 2.129 | 2.109 | 2.134 | 2.129 | 2.117 | 2.101 | |
| Rh-C5 | 1.993 | 1.967 | 1.891 | 1.880 | 1.997 | 1.894 | 1.962 | 1.866 | |
| C5-O1 | 1.131 | 1.140 | 1.167 | 1.179 | 1.132 | 1.169 | 1.141 | 1.184 | |
| P2-Rh-P1b | 81.63 | 81.46 | 83.05 | 82.64 | 81.94 | 83.10 | 81.17 | 82.33 | |
| C6-Rh-C5 | 84.74 | 86.50 | 86.89 | 88.77 | 85.39 | 88.17 | 86.95 | 88.62 | 86.20 |
| C6-Rh-P2 | 89.06 | 88.78 | 87.76 | 87.55 | 172.10 | 170.91 | 174.28 | 174.67 | - |
| C5-Rh-C2 | 173.53 | 175.10 | 173.95 | 176.01 | 102.42 | 99.73 | 98.78 | 96.67 | |
| C5-Rh-P1 | 104.55 | 103.24 | 102.28 | 100.98 | 175.13 | 164.68 | 176.04 | 144.85 | |
| C6-Rh-P1 | 170.67 | 170.19 | 170.79 | 169.98 | 90.24 | 88.12 | 93.06 | 93.75 | |

a bond distances are in A and bond angles are in b data for Rh-PMe3 c data for Rh-PF3

The HF/3-21G and HF/LANL2DZ levels give very poor results (the bond distances are about 0.1 Å and 0.2 Å from data as stated in the international table for X-Ray crystallography). The DFT/3-21G level also gives quite poor results (0.1Å and 0.06Å far from ITC). Although the for angles from HF/LANL2DZ level gives fairly agreement, the bond lengths are in poor agreement. The DFT/LANL2DZ result are in the most reasonable.²

Table 4.2 Energies of complexes 1.5 and 1.6.

| | HF/3-21G | HF/LANL2DZ | B3LYP/3-21G | B3LYP/ LANL2DZ | Unit |
|------------|-------------|-------------|-------------|----------------|----------|
| 1.5 | -5847.89758 | -5854.49991 | -629.75300 | -633.93920 | au |
| 1.6 | -5847.89731 | -5854.49786 | -629.74860 | -633.93357 | au |
| ΔE=1.5-1.6 | +0.00027 | +0.00205 | +0.00540 | +0.00664 | Au |
| | +0.1694 | +1.2864 | +3.3886 | +4.1667 | Kcal/mol |

1 au = 627.5095 kcal/mol

Here are the optimized energy results from calculation using Hartree-Fock method and Density Functional Theory. Complex 1.5 has energy different from complex 1.6 are 0.16, 1.29, 3.39 and 4.17 kcal/mols for HF/3-21G, HF/LANL2DZ, B3LYP/3-21G and B3LYP/ LANL2DZ respectively. As you can see, the Hatree – Fock energy with 3-21G and LANL2DZ basis sets give no significantly different between those two complex. It was only 0.16 and 1.28 kcal/mols. The calculating energy using DFT with 3-21G is about 3.39 kcal/mol. This is quite agreement, but give quite poor angle parameter (Table 4.1). Clearly, density function calculating energy with LANL2DZ basis set gives a good agreement, corresponding with the most reasonable data parameters.

In sum, the higher level gives the better results. The presented results indicate that B3LYP calculation with LANL2DZ basis set method was the best tool. Then, it use to model these and similar systems.

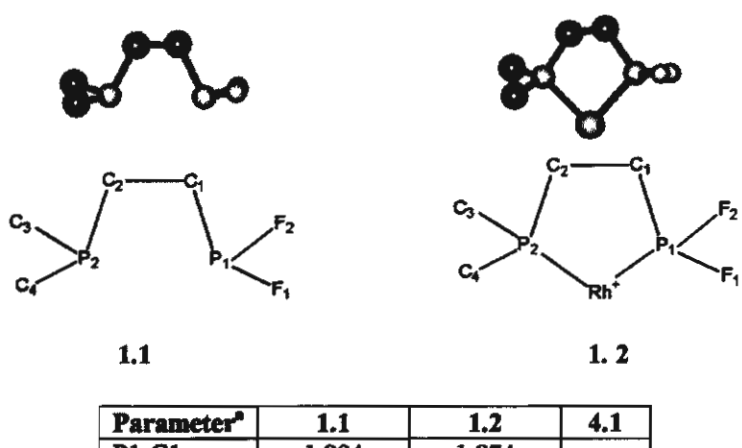
4.2 To Find the Most Stable Structure.

Perform geometry optimizations of these 6 structures illustrated below. Many for optimization steps need to converge the structures. The optimization was carried out on using density functional level with the LANL2DZ basis set.

4.2.1 The Study of Ligand 1.1 and Cation 1.2

Ligand 1.1 is the most important in this study. It is used as a promoter for the rhodium catalyst in the methanol carbonylation process.

Table 4.3 The optimized parameters of 1.1 and 1.2



| Parameter* | 1.1 | 1,2 | 4.1 |
|------------|------------|------------|-------|
| P1-C1 | 1.894 | 1.874 | • |
| P1-F1 | 1.745 | 1.724 | |
| P2-C2 | 1.923 | _ | • |
| C1-C2 | 1.542 | 1.552 | • |
| Rh-P1 | | 2,232 | 2.41 |
| Rh-P2 | - | 2.237 | 2.33 |
| P2-Rh-P1 | - | 106.10 | 86.20 |
| C2-C1-P1 | 112.60 | - | • |
| C1-C2-P1 | 113.27 | - | - |
| Rh-P1-C2 | - | 92.62 | - |
| Rh-P2-C1 | • | 91.98 | - |
| Energy | -371.15021 | -480.58348 | - |

^a bond distances are in A and bond angles are in °

The average P-F and P-C(H₃) bond lengths of ligand 1.1 are 1.894 Å and 1.745 Å respectively. It is the typical value.¹ The bite angle of 1.2 is about 106.10° which is smaller than the experimental value found in the X-ray structure of the compound [RhCOCl(Ph₂P-CH₂-P(S)Ph₂), 4.1 by Baker and his co-worker.³ The two carbon back bone distances of 1.1 is 1.542 Å which is not significant different from ligand such as Ph₂P-CH₂-CH₂-PPh₂.⁴ It is a typical for Csp³- Csp³ hybridization. However, the distances of backbone are quite different from the Ph₂P-CH₂-P(S)Ph₂⁵, Ph₂P-CH₂-P(O)Ph₂⁶ and Ph₂P-CH₂-P(NPh)Ph₂⁷ respectively.

Based on the DFT calculation, the average P-F bond length of asymmetric phosphine ligand 1.1 is about 0.149 Å shorter than the average P-Me bond length, indicating a strong electron withdrawing group of F. Fluorine is highly electronegative and wishes to obtain additional electron density. As electron-

withdrawing (electronegative) groups are placed on the phosphorous atom, the σ -donating capacity of the phosphine ligand tends to decrease. At the same time, the energy of the π -acceptor (σ^*) on phosphorous is lowered in energy, providing an increase in backbonding ability. The result fit well with the electronic property. A highest occupied molecular orbital (HOMO) has stronger lone pairs on PMe₂ than that on PF₂. The stronger electronic property on PF₂ is favored for a lowest unoccupied molecular orbital (LUMO) as shown in Figure 4.2.

Table 4.4 Some atomic charges of ligand 1.1

| Total | Atomic charge |
|-------|---------------|
| P1 | 1.0442 |
| F1 | -0.4752 |
| F2 | -0.4718 |
| C1 | -0.1873 |

| Total | Atomic charge |
|-------|---------------|
| P2 | 0.6005 |
| C3 | -0.1824 |
| C4 | -0.1889 |
| C2 | -0.1387 |

atomic charge of hydrogen is 0.000 au

The fluorine atom from PF₂ moiety is a significant site of negative charge, in contrast to a carbon atom from PMe₂ moiety. This results in an unequal charge distribute among the two phosphorus atoms and the two backbone carbons. The larger positive charge located on the phosphorus of PF₂ moiety while the other phosphorus is lower. The one backbone carbon, C1, bonded to PF₂ has more negative charge than C2, corresponding with the shorter P-C1 bonded. It attempts to draw electron from the two carbons which more closer together, in order to share the remaining electron more easily.² This can conclude that PF₂ is the lower of σ -donating, but the higher π -acceptor. This results also indicated by the molecular orbitals which shown in Figure 4.2.

By the consideration of the number of IR and Raman frequency, the stretching frequency number of PMe₂ moiety is higher than that of PF2 moiety. As known, the big number of frequency the better σ -donation.⁹

Table 4.5 Some numbers of IR and Raman stretching frequency of ligand 1.1

| Position | Frequency (cm ⁻¹) |
|----------|-------------------------------|
| P1 | 1.0442 |
| F1 | -0.4752 |
| F2 | -0.4718 |
| C1 | -0.1873 |

| Total | Atomic charge |
|-------|---------------|
| P2 | 0.6005 |
| C3 | -0.1824 |
| C4 | -0.1889 |
| C2 | -0.1387 |

The molecular orbitals and molecular orbital energies ligand 1.1 shown in Figure 4.3. The Highest Occupied Molecular Orbitals denotes as HOMO, HOMO-1 and HOMO-2 and the Lowest Unoccupied Molecular Orbitals denoted as LUMO and LUMO+1 are shown. The HOMO-2 show πC_{sp3} - πC_{sp3} on the backbone carbon. The other two HOMO show the lone pair electrons of the PMe2 and PF2 groups. The two LUMOs show anti-bonding orbitals: LUMO is a out of plane PF2 orbital and LUMO+1 is a in plane PF2 orbital. This confirms that PF2 is the stronger π -acceptor and the PMe2 is the good σ -donor.

The HOMO –LUMO gap energy is big (+0.2153 au). This is to confirm that this ligand is not a planar. 10-11

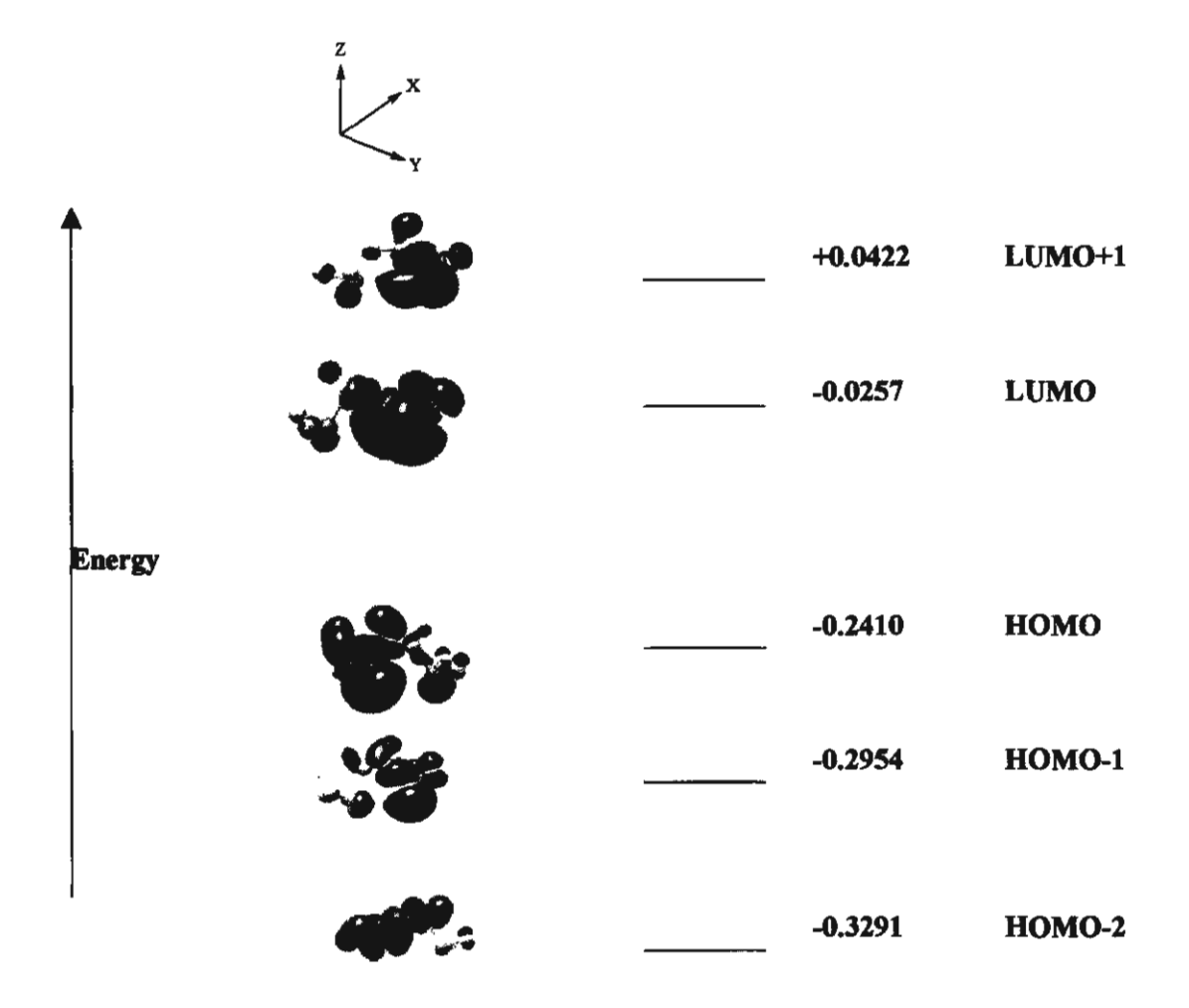


Figure 4.2 A symmetric ligand 1.1 shows the molecular orbitals. Hydrogen atoms are omitted for clarity. The energies are in au.

The molecular orbitals and molecular orbital energies cation 1.2 shown in Figure 4.3. The HOMO-2 and HOMO-1 show only d_{yz} and d_{xz} orbitals on the metal respectively. These two orbitals have no contribution from the asymmetric ligand 1.1. Whereas the HOMO show d_{xy} orbital. Clearly, it has the contribution from the PF₂ moiety of ligand 1.1. In other word, the pi- orbital from the LUMO of ligand 1.1 contribution to the HOMO of cation 1.2. The LUMO illustrates d_{x2-y2} orbital. Once again, it is clear to show the relation between metal and asymmetric ligand 1.1. whereas the other two LUMOs illustrate lone pair electrons and the pi-electron of metal center as shown in Figure 4.4. This is confirming the less electron on the metal center. It can conclude PF₂ is a greater π -acidity whereas PMe₂ is a greater σ -donation.

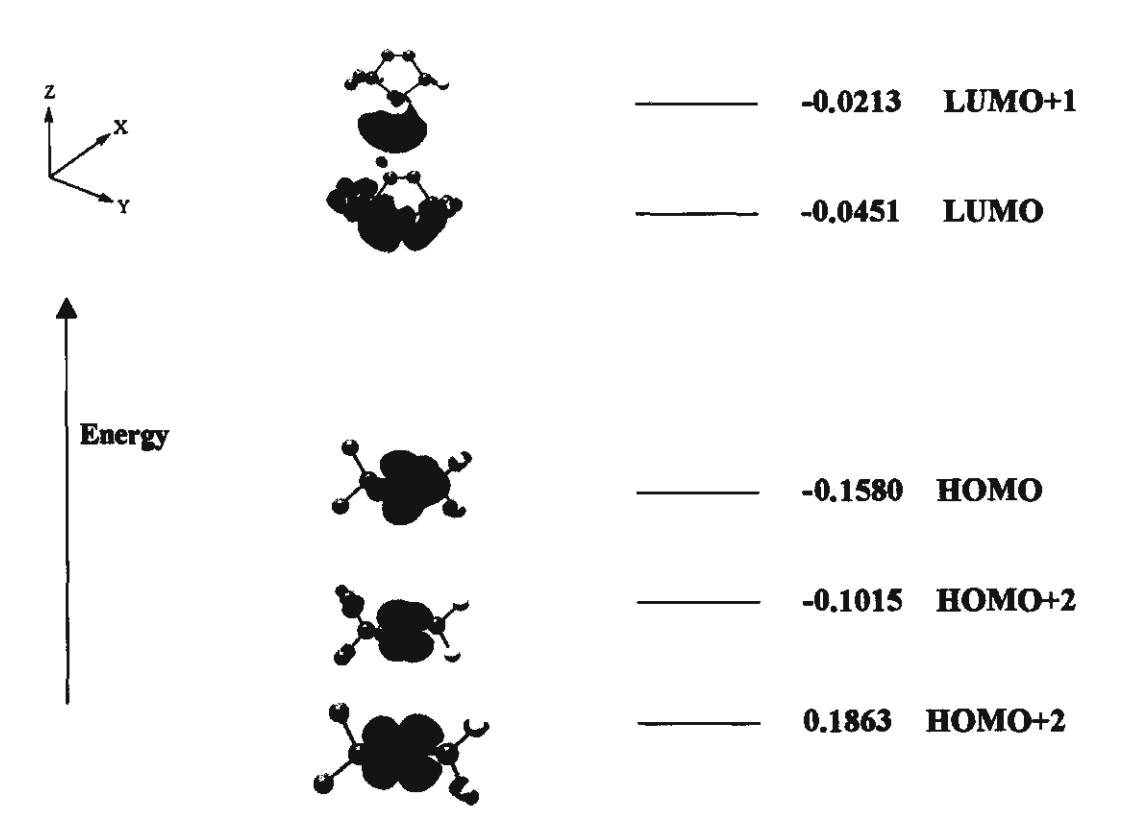


Figure 4.3 A rhodium cation 1.2 shows the molecular orbitals. Hydrogen atoms are omitted for clarity. The energies are in au.

In sum, ligand 1.1 is an asymmetrical diphosphine ligand which PF₂ moiety is strong electron withdrawing group and PMe₂ moiety is strong electron donating group, confirming by the number of stretching frequency, the bond distance and molecular orbital respectively. The molecular orbitals of cation 1.2 illustrate clearly how this ligand bonded to the metal center. This ligand may hope that it can generate more than one isomers, reasoning from the different groups (PMe₂ and PF₂). This would be favor the formation of different isomers when it promotes the organometallic catalyst complex, as shown.



Figure 4.4 The possible isomers generated by asymmetric diphosphine ligand 1.1

4.3 The Optimization of Four Rhodium Structures.

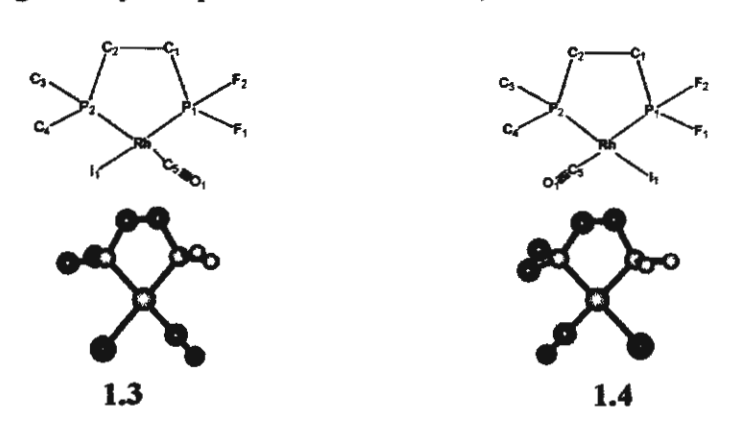
To find the most stable isomer from four rhodium complexes 1.3 1.4 1.5 and 1.6, the optimization is carried out on these isomers using DFT/LANL2DZ. The optimization data will compare to each other and to those relative structures.

The three sets of isomers were about to compared. The first set is isomers 1.3 and 1.4. Later is isomers 1.5 and 1.6. The final is the stable structures from first set and from the second set.

4.3.1 The Optimization of Isomers 1.3 and 1.4

Optimization is carried out on the isomeric species 1.3 and 1.4 using the DFT/LANL2DZ; the calculated optimization energies are given in Table 4.6.

Table 4.6 The geometry comparison of isomers 1.3, 1.4 and reference structures.



| Parameter* | 1,3 | 1.4 | ITC | 4.4 | 4.5 | 4.6 |
|------------|------------|------------|--------------------|-------|------|------|
| Rh-Pi* | 2.286 | 2.380 | 2.284 ^C | 2.34 | 2.41 | 2.27 |
| Rh-P2 | 2.442 | 2.405 | 2.219b | 2.29 | 2.33 | 2.48 |
| Rh-I1 | 2.709 | 2.706 | 2.749 | 2.84 | 2.80 | 2.79 |
| Rh-C5 | 1.898 | 1.871 | 1.912 | 1.81 | 1.89 | 1.85 |
| C5-O1 | 1.173 | 1.177 | 1.158 | 1.16 | 1.16 | 1.16 |
| P2-Rh-P1 | 83.42 | 82.76 | - | 85.47 | 91.4 | 88.8 |
| C5-Rh-P2 | | 93.76 | - | 94.4 | - | - |
| C5-Rh-P1 | 98.90 | - | 90.00 | 93.5 | 91.1 | - |
| Energy | -605.48109 | -605.46952 | - | - | - | - |

a bond distances are in A and bond angles are in b data for Rh-PMe₃ c data for Rh-PF₃

As regards optimized structures 1.3 and 1.4, the Rh-PMe₂ bond length in 1.3 is 0.037 A° longer than that in 1.4, indicating the stronger trans-directing CO over Γ. The Rh-PF bond length is 0.094A° shorter than that in 1.4. The Rh-I bond lengths in both structures are not significantly different and are in a good agreement with typical Rh-I distant. As one can see, in 1.3 the CO ligand weaken bond in trans position more than Γ. This is not different to the Rh-CO distance of [Rh(CO)IPh₂P(CH₂CH₂)PPh₂], 4.4. The Rh-I distance of 1.4 is slightly shorter than that in 1.4 but significant longer than those in similar structures [Rh(CO)IPh₂PCH₂PPh₂S], 4.5 and its isomer [RhI(CO)Ph₂PCH₂PPh₂S], 4.6. This is a consequence of less π-donating property of PF₂. The bite angle of 1.3 is 0.64°

smaller than that in 1.4 and is about 2.27° smaller than those in 4.4, 4.5 and 4.6 indicating less steric effect the lower energy as shown in Table 4.6.

The optimized free CO frequency is at 2313 cm⁻¹ with 1.143 A° of bond distance. This number is higher than experimental value which is the typical free CO frequency at 2143 cm⁻¹ with 1.128 A° of bond distance from the IR spectroscopy. Because of the nature of the computational involved, frequency are valid only stationary points on the PES. Raw frequency values computed at the DFT level contain systematic error due to the neglect of electron correlation, resulting in overestimates of about 10-10%. Therefore, it is usual to scale frequencies predicted at DFT level by empirical factor of 0.9623. Use of this factor has been demonstrated to produce very good agreement with experiment. For this calculation, it is about 200 cm⁻¹ higher which is the typical from such a calculation.²

Table 4.7 Number of IR and Raman CO stretching frequencies of series 1.

| CO | νCO | d (A) |
|--------------------|-----------|-----------|
| Free CO | 2143 | 1.128 |
| Terminal CO | 1850-2120 | 1.12-1.18 |
| Doubly bridging CO | 1700-1860 | • |

| structures | νCO | vC=O | d (A) | |
|------------|--------|------|-------|--|
| CO | 2313.0 | - | 1.143 | |
| 1.3 | 2000.4 | ** | 1.173 | |
| 1.4 | 1973.4 | - | 1.177 | |

By taking this theory into account, the number of IR and Raman CO stretching frequencies of isomers 1.3 at 2000.4 cm⁻¹ can observed which is higher than that of 1.4 at 1973.4 cm⁻¹. This number is typical for a terminal CO group.⁹ The calculated free CO distance is about 1.143 A° while the they are about 1.173 A° and 1.177 A° for structures 1.3 and 1.4. This is due too back donation. This occupation of the π^* on CO does lead to a decreased bond order in the carbon monoxide molecule itself. As we might expect, as the π -backdonation becomes stronger, the CO bond order should decrease from that of the free ligand. Two consequences that we might expect if the CO bond order was reduced would be a lengthening of the C-O bond and a decrease in the carbonyl stretching frequency in the IR. Both of these hold true as seen in Table 4.6. In other word, The more vCO stretching number is the weaker σ donation.

Optimization was carried out on the isomeric species 1.3 and 1.4 using DFT/LANL2DZ, the calculated optimization energies are given in Table 4.7.

Table 4.8 The energy of isomers 1.3 and 1.4

| Potential Energy (au*) | 1.3 | 1.4 | ΔE =1.3-1.4(au) | ΔE (kcal/mol) |
|------------------------|-----------|-----------|-----------------|---------------|
| DFT/LANL2DZ | -605.4811 | -605.4695 | -0.0116 | -7.28 |

The DFT/LANL2DZ calculated energies of complex 1.3 is lower than that in complex 1.4. This confirmed that complex 1.3 is more stable than complex 1.4.

The different energy (ΔE) values were used to calculated equilibrium constant. By using the equation of ΔG = -RT lnK, where ΔG is free energy change (kcal/mol), R is the gas constant (1.987 cal/mol/k), T is room temperature (298K) and K is equilibrium constant. Assuming that $\Delta G \sim \Delta H = \sim 7.28$ kcal/mol gives the ratio of 1.3:1.4 is ca. 218530:1.

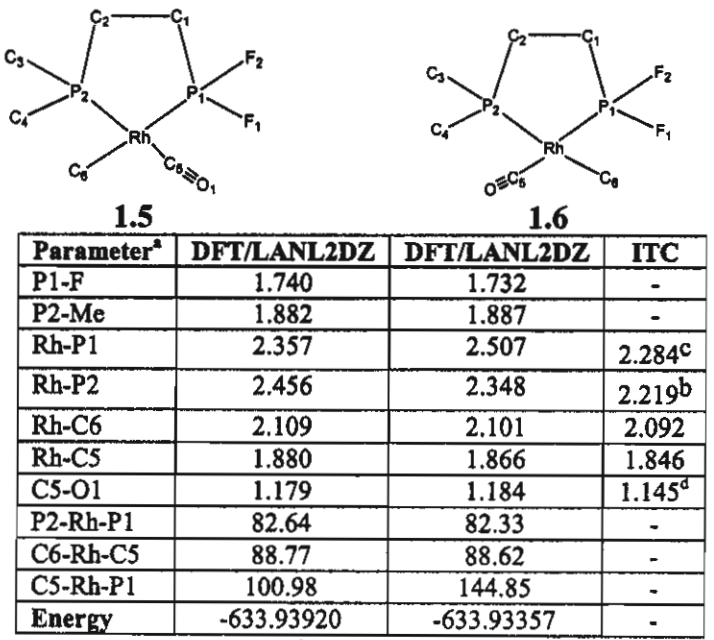
In sum, the computed structures confirm that the preferred stereochemistry at rhodium in which the $P(Me)_2$ is trans to the carbonyl and the $P(F)_2$ lies trans to the methyl group (isomer 1.3). The presence of the highly electronegative fluorine atoms in $P(F)_2$ makes the phosphorus a weak σ -donor but a stronger π - acceptor and the presence of methyl groups in $P(Me)_2$ makes it a stronger σ -donor but a weaker π -acceptor, consistent the variation in Rh-P bond lengths (Rh-PF₂ = 2.286 and Rh-PMe₂ = 2.442Å) and the number of IR and Raman stretching frequency.

4.3.2 The Optimization of Isomers 1.5 and 1.6

Once again, optimization was carried out on the isomeric species 1.5 and 1.6 using the DFT/LANL2DZ method. The calculated optimization energies are given in Table 4.8.

As regards optimized structures 1.5 and 1.6, the Rh-PMe and the Rh-PF bond length in 1.5 are 0.01 A° longer than that in 1.6. The Rh-CO distances in both structures are not different. This is a consequence of less π -donating property of PF₂. Surprisingly, the bite angle of 1.5 is 1.07° bigger than that in 1.5 and is in a good agreement with work done by Casey. 12

Table 4.9 The geometry comparison of isomers 1.5 and 1.6.



a bond distances are in Å and bond angles are in o b data for Rh-PMe3 c data for Rh-PF3 c data for free CO

However isomer 1.5 with Me trans to a good electron withdrawing group is preferred. However, isomer 1.5 is about 29 kcal/mol lower than in 1.3. These confirm that the presence of strong electronegativity fluorine atoms in PF₂ makes them weak σ -donors but much stronger π - acceptors and the presence of methyl groups in PMe₂ make them stronger σ -donors but much weaker π - acceptor. This is also indicated by the IR and Raman CO frequency numbers which are in the range of the terminal carbonyl group. However, the frequency number of 1.5 is at 1965.1 cm⁻¹ is higher

than that of 1.6 at 1934.8 cm⁻¹. This is corresponding with the slightly longer CO bond distance. In other word, the slightly longer C-O bond distance in 1.5 (1.179 Å) related to the lower C-O frequency (1916.1 cm⁻¹), indicating more Rh=C=O character.¹³

Results and Discussion-1

Table 4.10 The energy of isomers 1.5 and 1.6

Chapter 4

| Potential Energy (au) | 1.5 | 1.6 | ΔE =1.5-1.6(au) | ΔE (kcal/mol) |
|-----------------------|-----------|-----------|-----------------|---------------|
| DFT/LANL2DZ | -633.9392 | -633.9336 | -0.0056 | -3.51 |

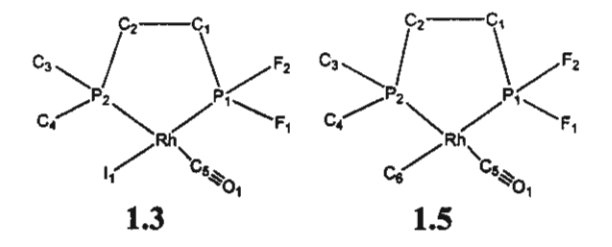
The value for complex 1.5 value is lower than 1.6 by \sim 3.51 kcal/mol, implying $\Delta G \sim \Delta H = -3.51$ kcal/mol and therefore a ratio of 1.5:1.6 is ca. 380:1. This confirms that complex 1.5 slightly is more stable than complex 1.6.

In sum, the preferred stereochemistry at rhodium in which the $P(Me)_2$ groups is trans to the carbonyl and the $P(F)_2$ lies trans to the methyl group (see Table 4.6). Once again, the presence of the highly electronegative fluorine atoms in $P(F)_2$ makes the phosphorus a weak σ -donor but a stronger π -acceptor and the presence of methyl groups in $P(Me)_2$ makes them stronger σ -donors but much weaker π - acceptor, consistent the variation in Rh-P bond lengths (Rh-PF₂ = 2.357 and Rh-PMe₂ = 2.456Å).

4.3.3 The Optimization Energy for 1.3 and 1.5

Optimization was carried out on the isomeric species 1.3 and 1.5 using the DFT/LANL2DZ method. The optimized parameters are shown in Table 4.10.

Table 4.11 The geometry comparison of isomers 1.3 and 1.5.



| Parameter* | 1.3 | 1.5 | ITC |
|------------|-----------|-----------|--------------------|
| P1-F | 1.735 | 1.740 | - |
| P2-Me | 1.881 | 1.882 | - |
| Rh-P1 | 2.286 | 2.357 | 2.284° |
| Rh-P2 | 2.442 | 2.456 | 2.219 ^b |
| Rh-C6 | - | 2.109 | 2.092 |
| Rh-C5 | 1.898 | 1.880 | 1.912 |
| C5-O1 | 1.173 | 1.179 | 1.158 |
| Rh-I1 | 2.709 | - | - |
| P2-Rh-P1 | 83.42 | 82.64 | 86.28 |
| Energy | -605.4811 | -633.9392 | - |
| CO freq. | 2004.1 | 1916.1 | - |

a bond distances are in A and bond angles are in o

The P-Me₂ bond distances of the two isomers 1.3 and 1.5 are about the same. That is because they are trans to the strong electron withdrawing CO group. The difference is on the Rh-PF₂ bond distance. The Rh-PF₂ bond lengths in 1.5 is about 0.07 A higher than that in 1.3, indicating the strong trans-effect CH_3 group over Γ .

The IR and Raman CO frequency numbers are in the range of the terminal carbonyl group. However, the frequency number of 1.3 is about 88 cm⁻¹ higher than that of 1.5. This is corresponding with the slightly shorter of CO bond distance. In other word, the slightly longer C-O bond distance in 1.5 (1.179 Å) related to the lower C-O frequency (1916.1 cm⁻¹), indicating more Rh=C=O character.

Table 4.12 The energy of isomers 1.3 and 1.5

| Potential Energy (au) | 1.3 | 1.5 | $\Delta E = 1.3 - 1.5 (au)$ | ΔE (kcal/mol) |
|-----------------------|-----------|-----------|-----------------------------|---------------|
| DFT/LANL2DZ | -605.4811 | -633.9392 | -28.4581 | 17857.73 |

The calculated optimization energies are given in Table 4.9. The value of complex 1.5 is lower than 1.3 by ~17857 kcal/mol. This can imply that 1.5 is more stable than 1.3.

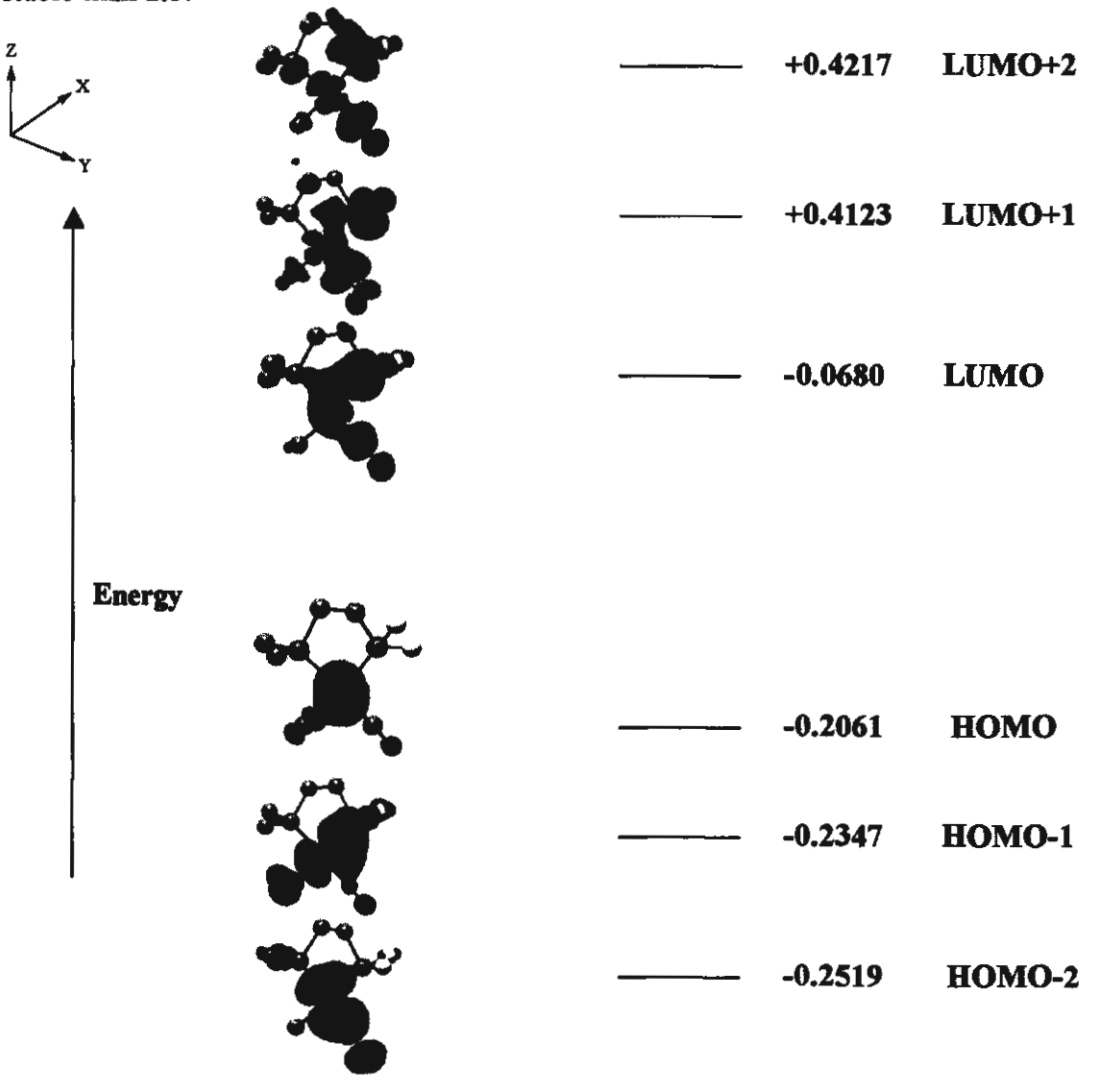


Figure 4.5 Some molecular orbitals of complex 1.5. Hydrogen atoms are omitted for clarity. The energies are in au.

To confirm the electronic effects at work, analysis of the molecular orbital is needed. The HOMO-2 show the d_{xy} -orbital with π bond on the C (O) and has no contribution from asymmetric ligand. While HOMO-1 show the d_{yz} -orbital with π bond on the C(H₃). The HOMO is a d_z^2 orbital and it is clear that the is has the contribution from the CH₃ group (σ -donation). while LUMO+1 is a d_x^2 - $_y^2$ -orbital. Clearly, the LUMO+1 show not only the Rh=C=O character, confirmed by the shorter Rh-C(O) bond distance (Table 4.10) but also the σ -donation of Γ , indicating by longer Rh-I bond distance. The LUMO+1 show also the π -bond on PF₂ moiety. The LUMO+2 shows the d_{xy} on metal with the Rh=C=O character or π - backbonding. The results from DFT/LANL2DZ are in a good agreement. The molecular orbital confirmed that the d_z^2 orbital is lower energy than d_x^2 - $_y^2$ -orbital as expected for a low-spin d_z^8 orbital Rh(I) configuration.

In sum, the rhodium complex 1.5 shows a cis-square-planar geometry with the bite angle of 82.64°. The computed all structures confirm that the preferred stereochemistry at rhodium in which the $P(Me)_2$ is trans to the carbonyl and the $P(F)_2$ lies trans to the methyl group. The presence of the highly electronegative fluorine atoms in $P(F)_2$ makes the phosphorus a weak σ -donor but a stronger π - acceptor and the presence of methyl groups in $P(Me)_2$ makes it a stronger σ -donor but a weaker π -acceptor, consistent the variation in Rh-P bond lengths. This is a consequence of the electron-donating properties of PMe_2 moiety, which is increase the electron density at the metal center and as a consequence the Rh to CO back bonding (more Rh=C=O character), indicating by the IR and Raman CO frequency number. This can confirm that isomer 1.5 is a good structure for such a series and as regards optimized energy, isomer 1.5 has the lowest energy from the all four rhodium complexes.

Although, isomer 1.3 is a higher calculated energy than 1.5. If the time permit, I will explore and it is worth to do full optimization on 1.3 as well. Chapter 4 48 Results and Discussion-1

4.4 To Do Full Optimization of Methanol Carbonylation Cycle (1.5)

In this section, isomer 1.5 is used as starting materials to do a full optimization for methanol carbonylation cycle. The work will be separated into two main parts. The first one is about all intermediate involving the cycle and the other one is about the four or five separate process, namely, oxidative addition, migratory insertion, ligand addition, reductive elimination and oxidative addition/reductive elimination respectively.

In the following, the structures and relative energies of all intermediates as well as their possible isomers are presented. Subsequently, the mechanism will describe of each elementary step of the catalytic cycle. Then the discussion of the gasphase-optimized geometries of the intermediates and relative energies of their isomers.

As noted in the introduction, no structural data on the intermediates 1.5, N, O and P of the methanol carbonylation cycle are available from the experimental data. For the species of 1.5, N, O and P have been proposed following a classical methanol carbonylation by Foster.¹⁴ several four-, five-, six- coordinate intermediate are involved. All intermediates are likely to exist in equilibrium of several isomers.

4.4.1 Initial Four-coordinated Complex 1.5

The initial four-coordinated complex is a 1.5. The interaction of CH₃I with the square planar complex 1.5 starts the catalyst cycle. This initial complex 1.5 has already discussed in Chapter 4. The optimized geometry parameters and relative energies are presented in Table 4.9.

4.4.2 Six-coordinated Complex N

The six-coordinated complex N is the product of CH_3I oxidative addition to the four co-coordinated reactant 1.5. There are five possible structures of complex N, denoted as N1, N2, N3, N4, N5 and N6 respectively. Isomers N1 and N2 still have a CO ligand where is trans to PMe₂ moiety and addition two anionic CH_3^- and Γ groups. The two anionic groups are in axial position. The difference of isomers N1 and N2 is only the opposite position of the two anionic groups. Isomer N1 has CH_3^- in the top and Γ in the bottom where this position is opposite in N2. Isomers N3 and N4 still have CH_3 ligand where trans to PF_2 moiety. These two isomers have CH_3^- and CO groups in an axial position. Once again, the difference of these two isomers is only the position of axial groups, inwhich are interchange. Isomer N5 is totally different from an original starting material 1.5. CO is opposite to Γ . Both CO and Γ of isomer N5 are in the axial position. The two CH_3 ligands are in a cis position. One CH_3^- is trans to the PMe₂ moiety whereas another is trans to PF_2 moiety. All structures and optimization energy are shown in Table 4.13 and in Appendix A.

Chapter 4 49 Results and Discussion-1

Table 4.13 The optimization energy and relative energy of complex N series.

| Complex | Structure | Structure | Energy (au) | Relative energy (au) | Relative energy (kcal/mol) |
|---------|-----------|---|----------------|----------------------------|----------------------------------|
| N1 | | C ₂ C ₂ C ₃ C ₄ C ₇ | -685.2561 | 0.0014 | 0.88 |
| N2 | XX | C ₄ | -685.2575 | 0.0000 | 0.00 |
| N3 | XX | C ₂ C ₃ C ₇ C ₇ F ₇ C ₈ C ₈ C ₉ | -685.2427 | 0.0148 | 9.29 |
| N4 | X | C ₃ C ₁ C ₁ F ₂ C ₁ F ₂ C ₃ C ₄ F ₁ C ₄ C ₅ C ₇ C ₈ C ₇ C ₉ | -685.1626 | 0.0949 | 59.55 |
| N5 | | C2 C1 P2 C1 P2 C2 C1 P2 C2 C1 P2 C2 C2 C1 P2 C2 | -685.2477 | 0.0098 | 6.15 |

The hydrogen atoms are omitted for clarity. 1 au = 627.5095 kcal/mol.

Based on the density functional optimization energy, isomers N1 and N2 are the most stable structures. The optimized N1 energy is about the same as the optimized N2 energy. The relative energy shows that N2 energy is about 0.88 kcal/mol different from N1 energy as shown in Table 4.12. It can be considered isomers N1 and N2 are isoenergetic. Isomers N3 and N5 is about 9.29 and 6.15 kcal/mol higher than that of N2 respectively. The energy difference of more than 5 kcal/mol for the latter is significant.² The significant energy different is for N4 indicating by the relative energy of 59.55 kcal/mol from the most stable conformation isomer N2.

The octahedral complexes of series N are only slightly distorted from the idea octahedral coordinate, indicating by bond angles around rhodium atom from each isomer. The asymmetric ligands results in a slightly difference in the two Rh-P distances. The Rh-PF₂ bond distance of the series N are not different as shown in Table 4.11. The big difference is on the Rh-PMe₂ bond distances inwhich are longer than those in 1.5, excepted in N5. IsomerN1 and N2 have the CO group trans to PMe₂ making the longer bond 2.463 and 2.472 A° respectively. Whilst the Rh-PMe₂ bond distances of N3, N4 and 4.4 are shorter than those in isomer N1 and N2. This can confirms the trans directing of Γ which is less than CO. The Rh-P bond distance 2.502A° of N5 is also indicative the less trans directing. As comparing the bond distance of complex N, the increasing of the bond elongatation of Rh-PMe₂ in trans position to the ligands in the series Γ> CO>CH₃. The Rh-I distance of isomer N1 and N2 are longer than those in isomer N3 and N4. It is a typical for groups in an axial position which are usually longer than those in equatorial. The iodide ligands I₂ of

isomer N1 and N2 are bent. As already noted, these structural features may be rationalized in terms of steric repulsive between the CO groups and I, making the bigger I-Rh-CO angles, 89.85 and 95.14°.

Table 4.14 The parameters of the N series with calculated bond distances (in A°) and bond angles (in deg°).

| Parameter* | N1 | N2 | N3 | N4 | N5 | 1.5 | 4.4 |
|------------|--------|---------|-------|-------|--------|--------|-------|
| Rh-P1 | 2.464 | 2.481 | 2.458 | 2.354 | 2.502 | 2.357 | 2.34 |
| Rh-P2 | 2.463 | 2.472 | 2.415 | 2.352 | 2.579 | 2.456 | 2.29 |
| Rh-C6 | 2.114 | 2.112 | 2.125 | 2.020 | 2.130 | 2.109 | • |
| Rh-C5 | 1.899 | 1.898 | 1.975 | 2.020 | 1.865 | 1.880 | 1.81 |
| C5-O1 | 1.171 | 1.171 | 1.172 | 1.115 | 1.174 | 1.179 | 1.16 |
| Rh-I2 | 2.902 | 2.913 | 2.784 | 2.580 | 2.834 | - | 2.84 |
| Rh-C7 | 2.129 | 2.125 | 2.144 | 2.020 | 2.118 | - | - |
| P2-Rh-P1 | 81.45 | 80.90 | 83.70 | 82.52 | 79.41 | 82.64 | 85.47 |
| C6-Rh-C5 | 88.78 | 89.51 | 89.73 | 87.51 | 87.67 | 88.77 | 94.4 |
| C6-Rh-P2 | 82.20 | 88.21 | 87.60 | 93.60 | 174.23 | 87.55 | 93.5 |
| C5-Rh-P2 | 175.02 | 176.79 | 97.50 | 88.77 | 98.09 | 176.01 | - |
| C5-Rh-P1 | 101.07 | 101.32 | 99.23 | 92.11 | 98.88 | 100.98 | - |
| C6-Rh-I2 | 94.84 | 86.1281 | | | | - | - |
| C5-Rh-I2 | 89.85 | 95.14 | 91.39 | 90.49 | 86.83 | - | • |

By consideration of the number of IR and Raman CO stretching frequencies, the frequency at 1934 cm⁻¹ of 1.5 can observed which is lower than free CO. This number is typical. The typical free CO frequency at 2143 cm⁻¹ with 1.128 A° of bond distance from the IR spectroscopy. For this optimized, the optimized free CO frequency is at 2313 cm⁻¹ with 1.143 A° of bond distance. It is about 200 cm⁻¹ higher which is the typical from such a calculation. After oxidative addition, the frequency of N₁ and N₂ can observed at about 2012 cm⁻¹ which are higher than that of 1.5, but is close to the X-ray crystal data of 4.5 with as appearance in (2010 cm⁻¹). The calculated free CO distance is about 1.143 A° while the they are about 1.171 A° for structures. This is due too back donation. This occupation of the π^* on CO does lead to a decreased bond order in the carbon monoxide molecule itself. As we might expect, as the π -backdonation becomes stronger, the CO bond order should decrease from that of the free ligand. Two consequences that we might expect if the CO bond order was reduced would be a lengthening of the C-O bond and a decrease in the carbonyl stretching frequency in the IR. Both of these hold true as seen in Table 4.15.

Table 4.15 Number of IR and Raman CO stretching frequencies of N series.

| СО | νCO | d (A) |
|--------------------|-----------|-----------|
| Free CO | 2143 | 1.128 |
| Terminal CO | 1850-2120 | 1.12-1.18 |
| Doubly bridging CO | 1700-1860 | - |
| N2 | 2011.6 | 1.172 |
| N3 | 1988.8 | 1.172 |

| structures | νCO | vC≔O | d (A) |
|------------|--------|------|-------|
| СО | 2313.0 | | 1.143 |
| 1.5 | 1934.8 | - | 1.179 |
| N1 | 2012.0 | • | 1.171 |
| N4 | - | - | 1.115 |
| N5 | - | - | 1.174 |

As we can see, the isomer N1 and N2 have 300 cm^{-1} lower than free CO. It is a typical. With each charge added to the metal center, the CO stretching frequency decreases by approximately 100 cm^{-1} . The lower $\nu(\text{CO})$ at 1988 of N3 indicate the more Rh=C=O character as shown in Figure 4.6.

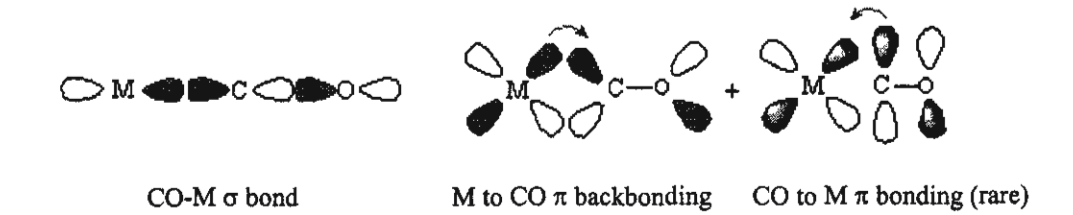


Figure 4.6 The relative of the three types (two of which are important) of CO-Metal bonding

As the electron density on a metal center increases, more π -backbonding to the CO ligand(s) takes place. This further weakens the C-O bond by pumping more electron density into the formally empty carbonyl π^* orbital. This increases the M-CO bond strength making it more double-bond-like, i.e., the resonance structure M=C=O assumes more importance. This can clearly be seen that illustrates the effect of charge (Rh(I) in 1.5 and Rh(III) in N1 and N2 as well as the electronegativity on the amount of metal to CO π -backbonding and the CO IR stretching frequency. The ability of the ligands on a metal to donate electron density to the metal center certainly has considerable effect on the absolute amount of electron density on that metal. This, in turn, naturally effects the ν_{CO} IR stretching frequencies in metal carbonyl complexes. Ligands that are *trans* to a carbonyl can have a particularly large effect on the ability of the CO ligand to effectively π -backbond to the metal.

In sum, all of these structures only slightly distorted from the idea octahedral coordinate. The coordinately unsaturated low spin d^6 complex resulting from the oxidative addition process of alkyl halide to square planar d^8 complex can adopt the octahedral conformations with the two anionic groups in the axial position. The isomers N2 and N1 are isoenergetic and are considered to be the most possible conformations. The geometry of strong trans-directing CO group is trans to the σ -donating PMe₂ moiety more favored over Γ whereas the weaker trans-directing CH₃ is trans to PF₂ moiety. The favored axial group are CH₃ and Γ groups. Based on ν CO IR stretching frequencies, the following ligands can be ranked from best π -acceptor to worst: CO > PF₃ > PR₃ > CH₃ > Γ

4.4.3 Five-coordinated Complex O

The five-coordinated complex O is the product of CO insertion into Rh-CH₃ bond type of N type complexes. As expected for the d^6 system, O exhibits a square-pyramidal structure. There are four possible structures, denoted as O1, O2, O3 and O4 with the Γ and the acyl in the apical position. The bond distance of the equatorial plane of complex O remained essentially unchanged to species of type N.

Isomers O1 and O2 have acyl group trans to PMe₂ moiety and anionic Γ is in the apical position. The isomers O1 and O2 are only different in the anionic group position. Isomer O1 has Γ in the top where this position is interchange in O2. Isomers O3 and O4 remain unchanged of rhodium complex 1.5 with the acyl group in the apical position. Once again, the different of these two isomers is only the position of apical groups, which are interchange. The energies and relative energies of all structures show in Table 4.16 and in Appendix B.